Low Temperature Soot Regime of Propane/Air in a Micro Flow Reactor with Controlled Temperature Profile

by

Abdul Hannan Khalid

A Thesis Presented in Partial Fulfillment
of the Requirements for the Degree
Master of Science

Approved June 2019 by the
Graduate Supervisory Committee:

Ryan Milcarek, Chair
Werner Dahm
Jeonglae Kim

ARIZONA STATE UNIVERSITY

August 2019

ABSTRACT

Micro/meso combustion has several advantages over regular combustion in terms of scale, efficiency, enhanced heat and mass transfer, quick startup and shutdown, fuel utilization and carbon footprint. This study aims to analyze the effect of temperature on critical sooting equivalence ratio and precursor formation in a micro-flow reactor. The effect of temperature on the critical sooting equivalence ratio of propane/air mixture at atmospheric pressure with temperatures ranging from 750-1250°C was investigated using a micro-flow reactor with a controlled temperature profile of diameter 2.3mm, equivalence ratios of 1-13 and inlet flow rates of 10 and 100sccm. The effect of inert gas dilution was studied by adding 90sccm of nitrogen to 10sccm of propane/air to make a total flow rate of 100sccm. The gas species were collected at the end of the reactor using a gas chromatograph for further analysis. Soot was indicated by visually examining the reactor before and after combustion for traces of soot particles on the inside of the reactor. At 1000-1250°C carbon deposition/soot formation was observed inside the reactor at critical sooting equivalence ratios. At 750-950°C, no soot formation was observed despite operating at much higher equivalence ratio, i.e., up to 100. Adding nitrogen resulted in an increase in the critical sooting equivalence ratio.

The wall temperature profiles were obtained with the help of a K-type thermocouple, to get an idea of the difference between the wall temperature provided with the resistive heater and the wall temperature with combustion inside the reactor. The temperature profiles were very similar in the case of 10sccm but markedly different in the other two cases for all the temperatures.

These results indicate a trend that is not well-known or understood for sooting flames, i.e., decreasing temperature decreases soot formation. The reactor capability to examine the effect of temperature on the critical sooting equivalence ratio at different flow rates was successfully demonstrated.

ACKNOWLEDGMENTS

I would like to extend my gratitude to Dr. Ryan Milcarek for giving me this opportunity to work with him on this project. I would like to thank him for his dedication and support throughout this time. I would also like to thank Dr. Werner Dahm and Dr. Jeonglae Kim for being a part of my thesis committee. I would like to thank ASU's MORE funding program which helped to partially fund this research. Thanks to my colleagues Jiashen Tian, Rhushikesh Ghotkar and Brent Skabelund for their continuous support during experimentation.

DEDICATION

First and foremost, I would like to thank the Almighty God for giving me the courage and constant spiritual support. I would like to extend my profound gratitude to my parents and siblings for their constant support to my endeavors ever since. I would like to thank all my friends who have been a source of great motivation and support throughout.

TABLE OF CONTENTS

LIST OF TABLES

LIST OF FIGURES

Figure Page

CHAPTER 1

INTRODUCTION

Ever since the inception of combustion engines, emissions have been a severe problem, posing serious threats to the environment and humans equally. The increasing amount of soot emissions in the environment has been a major cause of carcinogens absorption, which in turn pose serious health risks [1]. Efforts have been made to reduce these emissions to preserve the integrity of the atmosphere for a sustainable future. Furthermore, soot formation results in decreased efficiency of combustion based systems which results in more hydrocarbon usage and further emissions. Generally, the carbonaceous particles that are the products of gas phase combustion are called soot which is markedly different from coke or cenospheres developed by the pyrolysis of liquid hydrocarbon fuels. Hydrogen is an integral part of the soot particles formed in flames which often consists of 1% hydrogen by weight that corresponds to an empirical formula of C_8H [2].

Under stoichiometric conditions, combustion of hydrocarbons ideally yields only carbon dioxide and water which is accompanied by maximum heat generation. However, combustion usually doesn't take place under these perfectly ideal conditions. The application dictates if there is a need to burn at fuel-lean or fuel-rich conditions. In ultra-lean regime production of VOCs is promoted thus producing more pollutant species. In ultra-rich regime, where there is a sparse amount of oxidant, the mixture can be converted efficiently into syngas due to incomplete oxidation of hydrocarbon fuel. This incomplete combustion results in the formation of carbon monoxide, carbon dioxide, hydrogen, soot precursors (PAH) and soot.

The overall stoichiometric reaction can be written as

$$C_nH_m + \left(n + \frac{m}{4}\right)(O_2 + 3.76N_2) \rightarrow nCo_2 + \frac{m}{2}H_20 + 3.76\left(n + \frac{m}{4}\right)N_2$$

Hence, stoichiometric air/fuel mass ratio is

$$\left(\frac{air}{fuel}\right)_s = \left(\frac{m_a}{m_f}\right)_s = \frac{\left(n + \frac{m}{4}\right)(32 + 3.76 * 28)}{n.12 + m.1} = 137.28\frac{n + \frac{m}{4}}{12n + m}$$

And, stoichiometric fuel/air mass ratio is

$$\left(\frac{fuel}{air}\right)_s = \left(\frac{m_f}{m_a}\right)_s = \frac{n.12 + m.1}{\left(n + \frac{m}{4}\right)(32 + 3.76 * 28)} = .007284\frac{12n + m}{n + \frac{m}{4}}$$

Stoichiometric fuel mass fraction can be written as

$$\left(\frac{m_f}{m_f + m_a}\right) = \left(\frac{1}{1 + \left(\frac{m_a}{m_f}\right)_s}\right) = \frac{12n + m}{149.28n + 35.32m}$$

Equivalence ratio is defined as

$$\Phi = \frac{\left(\frac{\mathrm{m_f}}{\mathrm{m_a}}\right)_{\mathrm{actual}}}{\left(\frac{m_f}{m_a}\right)_{stoic}}$$

Based on equivalence ratio, we can now define the stoichiometric, fuel-lean and fuel-rich combustion as under;

- Stoichiometric combustion: $\Phi = 1$
- Fuel-lean combustion (excess air remains): $\Phi < 1$
- Fuel-rich combustion (excess fuel remains): $\Phi > 1$

This fuel-rich combustion is particularly important in fuel cells because they need hydrogen rich syngas to have higher efficiencies [3]. An electrochemical process

efficiently converts the fuel directly into electricity in a fuel cell, which is not limited by thermodynamic Carnot cycle efficiency. One of the major issues which severely limits fuel cell technology is the production, storage, and transportation of fuel sources, i.e., hydrogen has a high energy density (>1478Wh/L) at 700bar and low energy density (3.3Wh/L) at atmospheric conditions. As maintaining high pressure like 700 bar is very difficult and the low energy density at atmospheric conditions renders hydrogen a poor candidate to utilize, we can easily get hydrogen-rich syngas by combusting hydrocarbon fuels under fuel-rich conditions "on-demand" basis. Thus, hydrocarbon fuels at atmospheric conditions can act as a hydrogen carrier thus eliminating the need to store hydrogen at elevated pressures.

Soot is an undesirable by-product of combustion in some cases, i.e., soot deposition is problematic for the performance of a combustion system. In the regenerative cooling method, soot deposition on channel walls occurs because of endothermic fuel cracking used to mitigate the effect of high-temperature combustion temperature of the chamber walls [4]. A large amount of soot and PAH are produced due to endothermic pyrolysis of fuel-rich mixture, which in turn can clog the cooling channel thus inhibiting heat transfer [4].

Soot precursors and PAH have carcinogenic and mutagenic properties. They can easily be absorbed on to the soot particles which is considered a hazardous pollutant due to its miniature size. It has been shown that these fine particles having a diameter less than 2.5μm are the root causes of several respiratory ailments like bronchitis, asthma and reduced lung functions [1]. Longer exposure may cause lung cancer. Also, the residence time of soot particles in the atmosphere depends on their diameter. Depending on diameter, the soot particles can stay up to a week in the

atmosphere which increases their exposure to PAH which gets absorbed on their surface thus posing health treats. Also, these fine particles are more likely to go from the lungs to the blood and other body parts posing serious health threats [5]. The excessive emissions and longer residence time of soot particles in the atmosphere also promote global warming, i.e., soot particles are essentially black bodies which tend to absorb solar radiation readily giving positive heat feedback to the atmosphere. Similarly, when soot particles deposits on the snow, they tend to accelerate the heat absorption due to radiation as well as affect the albedo of snow cover, accelerating melting [6].

The major source of soot in the atmosphere is combustion, be it IC (internal combustion) engines, jet engines or an industrial furnace. As a result, there is a need to investigate possible soot mitigation techniques for a sustainable future. Recently, low temperature (<1000°C) combustion via micro-combustion has been identified as a possible means of reducing soot emissions and needs further investigation. In this research, we are going to further investigate the low temperature soot mitigation techniques.

Recently Maruta et al. [7] successfully demonstrated soot and PAH formation processes for methane and acetylene in a micro flow reactor with a controlled temperature profile. The dependency of soot formation limit on equivalence ratio and flow velocity (residence time) were identified. Also, temperature dependence of soot precursors was obtained at long residence time and a temperature ranging from 327-727℃. It was observed that the soot precursor molar concentrations increase as the temperature increases from 327℃ to 727℃. Milcarek et al. [8] studied the temperature dependence of soot formation for propane for an equivalence ratio 1-5.5

using a micro flow reactor as a fuel reformer. They observed no soot in the temperature range 750-900℃ for equivalence ratios 1-5.5, while soot formation was observed at 950℃ and 1000℃ at equivalence ratios above 2.5. Moreover, the syngas concentration in the exhaust was a strong function of temperature. At an equivalence ratio of 3, increasing temperature from 750℃ to 900℃ increased the syngas concentration from 2.3mol% H_2 and 10.7mol% CO to 9.2mol% H_2 and 15.3mol% CO. Increasing temperature further to 950℃ and 1000℃ didn't change the syngas concentration much and soot generation occurs.

To date, there has not been a lot of work to investigate soot formation at low temperature in a micro flow reactor. Operating at lower temperature has myriad benefits when it comes to fuel cell applications. This work aims to investigate the micro flow reactor for conditions where soot can be avoided. The aim is to operate at a higher equivalence ratio for more syngas generation and at a temperature that will reduce soot formation.

CHAPTER 2

LITERATURE REVIEW

This chapter includes the literature review which forms the basis for this thesis as well as presents a historical perspective on the problem. It starts with a brief introduction to micro/meso scale combustion and its application. Then a brief insight into soot and soot formation processes, i.e., chemical mechanisms as well as sooting tendencies. Then some soot mitigation techniques are briefly discussed which includes, but is not limited to:

- Oxidation
- Ionization
- Additives

While studying soot and its evolution in a micro-reactor, it is very important to characterize soot to better understand the physics behind the particle formation and growth during combustion. The "Experimental Techniques" chapter briefly discusses some of the current state of the art techniques being employed to study these phenomena.

2.1 Micro-combustion

Micro-combustion is a sequence of exothermic chemical reactions between a fuel and an oxidizer which is accompanied by the conversion of fuel/oxidizer mixture to carbon dioxide and water (under stoichiometric conditions) at a micro level. The small-scale nature of micro-combustion makes the wall interactions with flame as well as the molecular diffusion with a very low residence time of greater importance. A brief introduction of these two effects is discussed below.

Microchannels have a typical dimension which is usually less than the quenching distance, i.e., 1mm or less [9]. While meso-scale channels have a characteristics dimension greater than 1mm [9]. These characteristic dimensions are greater than the mean free path of hydrocarbon molecules under usual combustion condition. Thus, the Knudsen number, defined as the ratio of the mean free path to the characteristics dimension, is low enough for it to remain in the continuum regime of fluid mechanics. Micro-combustion does have a couple of issues that should be addressed before it becomes a viable option of energy extraction. Flame stabilization is very important for a sustained operation because of enhanced heat and mass transfer, which decreases the residence time for complete combustion. This limits the power extraction from the fuels due to incomplete combustion as well as the production of a higher fraction of pollutants like soot. The fuel/oxidizer's ability to sustain flame propagation strongly depends on the relative reactions rates as well as the heat generated and lost due to the higher surface-to-volume ratio. As the surface area-to-volume ratio increases substantially in micro-flow channels, the ratio of heat loss to the heat generated increases causing flame and radical quenching, which is undesirable for sustained operation. Davy demonstrated a quenching distance of 1mm.

Usually, in microscale combustion, Reynold's number is small, which implies the flow remains in the laminar flow regime. Since turbulent mixing doesn't happen in laminar flames, molecular diffusion is the primary mechanism for mixing. While in mesoscale, the flow might reach the turbulent transition regime because of a larger length scale. Turbulent mixing can happen which leads to better mixing and thus improving stability limits in meso-scale combustion [9].

Advances in the field of combustion at micro/meso scale during the past decade made it viable to be used in cogeneration of heat and power. Micro-combustion has application in portable electronics, sensors, actuators, rovers, robots, UAV's, thrusters as well as micro heating devices. It has the potential to help alleviate the declining hydrocarbon fuel resources and their large carbon footprint. Micro-combustion has several advantages over regular combustion. It is no longer governed by bulk behavior as surface interaction is a major driver. Micro/meso scale provides faster startup and shutdown, enhanced efficiencies and faster heat and mass transfer. Power generation by micro-reactor is advantageous because it is usually free from the frictional losses incurred by the piston in regular combustion engines. Liquid hydrocarbons have a high energy density, which can be extracted at small scales using micro-combustion which can replace batteries from traditional systems.

Maruta et al. [7] successfully demonstrated the use of a micro-reactor (∅=2mm) with a controlled temperature profile to study soot and its precursors for methane. They studied the temperature dependence of soot and its precursors. The soot luminosity acted as an indicator for soot inception. Milcarek et al. [8] also studied the temperature dependence of soot formation for propane with an equivalence ratio 1-5.5 using micro-flow reactor(∅=3.6mm) as a fuel reformer.

The micro-flow reactor has an inherent advantage of size, which allows strong coupling of the wall temperature and the reaction temperature. In other words, it allows for better control of the reaction temperature and hence the soot formation because soot formation is a strong function of temperature as indicated by Maruta et al. [7], Frenklach et al. [10] and Koki et al. [11]. These studies provide a strong basis

to use the micro-flow reactor to study sooting limits of fuels and temperature dependence of soot inception and growth phenomenon.

2.2 Soot

Generally, the carbonaceous particles that are the products of gas-phase combustion are called soot which is markedly different from coke or cenospheres developed by the pyrolysis of liquid hydrocarbon fuels. Hydrogen is an integral part of the soot particles formed in flames which often consists of 1% hydrogen by weight that corresponds to an empirical formula of C_8H[2]. It consists of almost spherical particles nipped together like pearls on a necklace with a diameter ranging from 100 to 2000 Å. Each particle consists of 10^4 crystallites and each of them consists of 5-10 carbon sheets which in turn consists of 100 carbon atoms and roughly have a length of 20-30Å. Soot can be quantified in terms of total volume fraction q~ (cm^3 soot/cm^3), the number of soot particles, N, (cm^{-3}) and the size of the particles, d, which are mutually dependent.

These carbonaceous soot particles have both detrimental and beneficial effects in the overall operation of the system. The presence of carbon particles increases the radiative power of the flame which is useful to enhance heat transfer. It eliminates the need for heavy heat exchanger equipment which is cost effective and reduces the complexity of the system. Hydrocarbon diffusion flames are luminous beyond the critical sooting equivalence ratio, which is due to the presence of carbon particles. These particles are essentially black bodies and radiate strongly due to high combustion gas temperature. The onset of luminosity is an indication of soot formation, which is highly emissive compared to the gaseous species. In many

industrial applications where heat transfer is a major concern, the system is operated in diffusion flame mode beyond the critical sooting limit to ensure maximum particulate formation which maximizes heat transfer. To meet emission standards, these particles can later be burned off/oxidized by additional air [4].

On the other hand, the soot particles in gas turbine engines can severely affect the lifetime of the blade [12]. Sooting in a closed combustion cycle system can clog the channels. Soot can absorb carcinogenic materials posing serious health risks to the environment and the population [1]. The general soot formation processes are discussed in the next section.

2.3 Soot Formation Processes

Soot formation is a very complex phenomenon. There are a lot of parameters that govern the soot formation process. As a result, it can be difficult to quantify soot based on some given parameters. Soot formation depends on the fuel type, H/C ratio, combustion process, combustion temperature, and flame type, among others. Much work has been done in the past to determine the relative tendencies of the hydrocarbon fuels to soot. Efforts have been made to come up with an acceptable explanation of why these tendencies exist and how to limit particulate formation during the combustion process to meet the emission standards of a particular system.

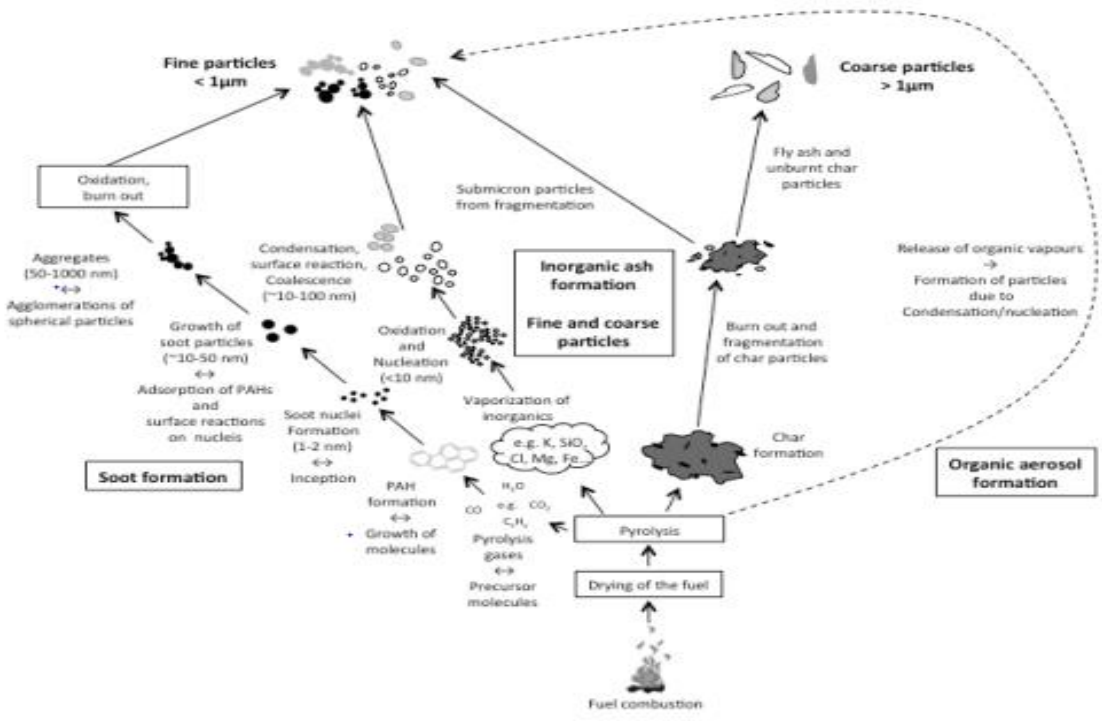

Figure 1: Description of particles formation via various production paths [50].

As shown in Fig. 1, the first condensed phase arises from the fuel molecules via their pyrolysis, which includes various unsaturated hydrocarbons particularly acetylene and its higher analogs as well as PAH which are generally considered precursors for soot formation [50]. The first nuclei (d<20 Å) forms by the condensation of gas-phase species. After the inception of first nuclei, PAH starts condensing on the solid phase nuclei which is the process by which surface growth occurs [13]. Growth leads to an increase in soot, but the number of particles N remains the same. As evident from Fig. 2 where the molecular weight is plotted against hydrogen mole fraction [51]. The final soot is formed by either condensation of species on the incipient nuclei with right hydrogen content or with higher hydrogen content which is then followed by dehydrogenation. So conclusively, neither polyacetylene chain or PAH would lead to soot which has hydrogen mole fraction in the range of .1-.2. These

individual particles also coagulate whereby N (number of particles) decreases and q (volume fraction) increases. Particle growth is essentially the result of these two phenomena occurring simultaneously which is followed by oxidation, forming CO and CO_2.

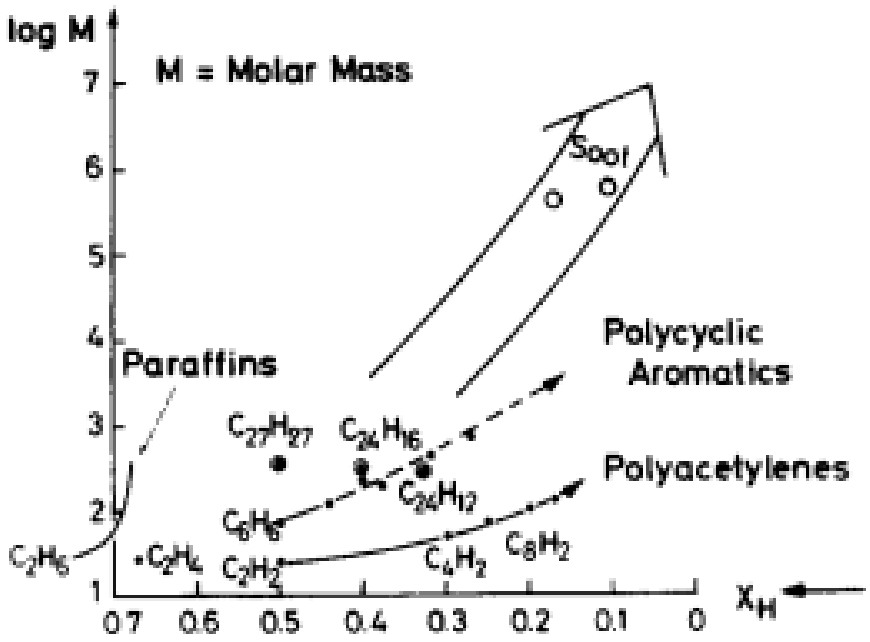

FIG. 1. Pathways to soot formation.[10]

Figure 2: Pathways to soot formation [51].

The particles emitted can be oxidized by an afterburner in the presence of excess oxygen. Whether the fuel is aromatic or nonaromatic greatly impacts early nucleation and ultimately the soot. Generally aromatic tend to have higher sooting tendencies due to a cyclic group already present which are easily converted into a polynuclear aromatic structure. For nonaromatic fuels, precursors undergo cyclization to form an aromatic ring which grows into PAH due to soot precursors such as acetylene. This aromatic structure then develops into particle's nuclei which contains a large amount

of hydrogen which eventually dehydrogenates due to high combustion temperature while absorbing PAH and growing, eventually forming the final soot structure.

2.4 Sooting Tendencies

Sooting tendencies generally referred to as the "qualitative or quantitative measure of the incipient soot particle formation and growth rates of one fuel relative to another in a particular experimental combustion configuration". These tendencies are also a strong function of the combustion process under investigation. For instance, in premixed flames, there is a competition between soot precursor formation and their oxidation, but no oxidation occurs during fuel pyrolysis in diffusion flames.

The sooting limit is defined thermodynamically by

$$C_m H_n + yO_2 \rightarrow 2yCO + \frac{n}{2}H_2 + (m - 2y)C_s$$

When m becomes larger than 2y, i.e., when the C/O ratio exceeds unity meaning when the number of carbon atoms in fuel exceeds the total number of oxygen atoms in the oxidizer, then there are no oxygen atoms to oxidize additional carbon atoms which are essentially soot [14]. However, experimentally sooting occurs at C/O=.5 [14]. One of the explanations for this may be the fact that significant amount of CO_2 and H_2O are present even beyond the critical C/O ratio which results in low sooting limit because not all the oxygen atoms are available for soot oxidation. The OH radical reacts with H_2 and CO to produce H_2O and CO_2.

$$CO + OH \leftrightarrow CO_2 + H$$

$$H_2 + OH \leftrightarrow H_2O + H$$

To reduce carbon dioxide and water to CO and OH requires high activation energy which explains the occurrence of soot at a lower C/O ratio. Increasing

temperature also increases the sooting limit by promoting the reverse reaction thus liberating more OH radicals for soot oxidation. The critical sooting limit is also weakly pressure dependent and dilution at a constant temperature. However, dilution doesn't have a large effect on the sooting limit.

The soot inception is generally defined by the onset of yellow luminosity which is in turn related to the critical equivalence ratio. The higher the critical sooting equivalence ratio, the lower the tendency to soot. The trend observed for premixed flames is [57,58]

Aromatics > Alkanes > Alkenes > Alkynes

Also, the equivalence ratio can be correlated with the number of C-C bonds in the fuel, which shows that the critical equivalence ratio decreases as the number of C-C bonds increases. That implies that the specific fuel structure is irrelevant when determining the sooting tendency under premixed condition, i.e., at same flame temperature benzene (C_6H_6) has the same sooting tendency as decane ($C_{10}H_{22}$) because they both have almost same number of C-C bonds. Which leads to the conclusion that all fuels break down essentially to the same species which develops into soot particles. The temperature dependence of sooting tendencies was studied by Milliken [68], who found that the cooler the flame, the greater is the tendency to soot, i.e., lower critical equivalence ratio. There are two competing processes occurring simultaneously in a sooting flame: the pyrolysis rate of precursors and their oxidation by OH group. When the temperature is increased, the oxidative attack rate increases faster than the pyrolysis rate of precursors formation, thus diminishing the tendency of flame to soot.

Soot yield isn't always correlated with the critical C/O ratio, i.e., n-hexane and benzene both have the same critical C/O ratio of 0.5, but at C/O ratio of 0.8, benzene

produces 10 times more soot than n-hexane. Also, the comparison between benzene and ethylene flame shows that despite the fact that benzene has higher critical C/O ratio (0.65) than ethylene(0.60), soot volume fraction at C/O=0.72 from benzene is three times that of ethylene (Fig. 3) [15]. Soot yield is a strong function of pressure mainly due to enhanced absorption and condensation on the soot particles at higher pressure. But pressure doesn't affect critical C/O ratio because surface growth needs some incipient particle to grow on. Soot yield decreases with an increasing temperature near the critical C/O ratio because increasing temperature increases the oxidation rate of soot more than the soot formation rate. Beyond the critical C/O ratio, i.e., fuel-rich conditions, increasing temperature increases soot yield because of the increased pyrolysis at high temperature [16].

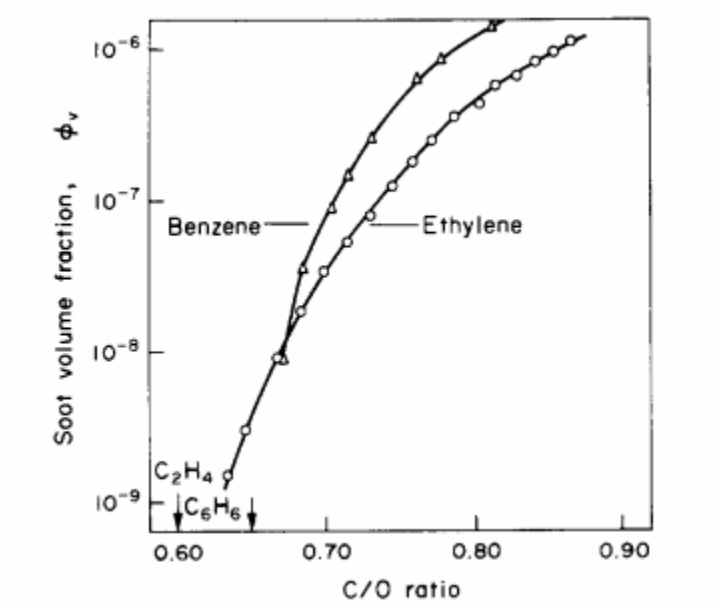

Figure 3: Comparison of soot loadings from ethylene and benzene air flames for a range of C/O ratios [15].

To get insight into the detailed soot formation process, chemical and physical measurements of temperature, velocity, laser extinction, scattering, and fluorescence

are necessary for premixed flames [84,85]. They concluded that the surface growth in aliphatic hydrocarbons is related to the dominant role played by acetylene because it's the main constituent of post-flame gases. Aromatic fuels have almost 1000 times more PAH than aliphatic fuels in their post-flame region.

2.5 Chemical Mechanism of Soot Formation

A lot of studies suggest that there are essential underlying mechanisms in soot formation process that are modified only with respect to some alternate routes to intermediates, which are dependent on the general characteristics of fuel, temperature as well as the combustion system. This means that the initial rate of ring formation determines the relative tendencies of different fuels to soot. Thus, the incipient soot particle concentrations essentially determine the total amount of soot formed [98].

Colket suggested that acetylene addition to the n-butadienyl radical (C_4H_5) during pyrolysis forms the final benzene ring as shown by the first path in Fig. 4. Additionally, in the same temperature regime, another route B to ring formation is through vinyl radical addition to vinylacetylene. The incipient soot formation is determined by the fastest route which forms the intermediates for the ring formation mechanism. As a result, fuels whose pyrolysis more readily forms the butadienyl radical have a higher propensity to soot, i.e., C4 hydrocarbons can easily form butadienyl, so they have a greater propensity to soot. The sooting tendency of butene is greater than acetylene because it creates butadienyl radical more easily. Similarly, the tendency of butadiene is greater than butene because it can form butadienyl radical more easily.

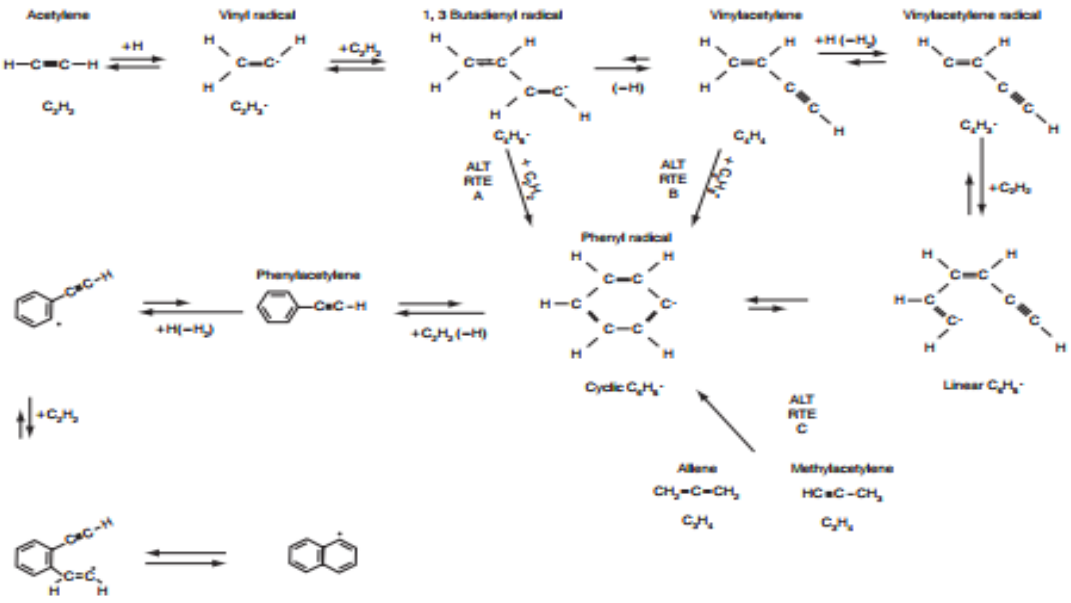

Figure 4: Reaction paths to benzene ring formation.

Detailed analysis of the above diagram shows the relative importance of the pyrolysis and significance of H atoms and acetylene concentration which by far are the most important species, other than butadienyl radical, to regulate the soot growth mechanism mainly by hydrogen abstraction and acetylene addition (HACA) [17].

2.6 Soot Mitigating

Lately, a lot of efforts has been done to reduce soot during combustion due to its undesirable properties. Some of these techniques are discussed below.

2.6.1 Oxidation

The soot particles can be oxidized before their exit from the combustion chamber which is a very difficult process to follow experimentally. Hynes et al. suggested that oxidation is the main driving force behind the difference in the soot particles actually formed in the combustion process and the particles emitted out of the combustion chamber [18]. Millikan stated that soot formation starts only after the

concentration of OH has approached its equilibrium value. OH is assumed to be the primary species to consume soot precursors as well as particles through their oxidation reaction. These oxidation reactions are accelerated at high temperature due to reverse reaction of CO_2 and H_2O to form CO, H and OH which in turn decreases the rate of HACA mechanism due to the liberation of hydrogen thus inhibiting soot inception by HACA [19]. Under fuel-rich conditions, hydroxyl radical is known to be a major oxidizing species [20]. In an ethylene/air flame at 1atm, Millikan identifies a dark zone prior to the soot formation region, rich of OH radical concentration. The appearance of the dark region was attributed to the consumption of precursors by the hydroxyl radical. Later it was confirmed that the OH radical is the main oxidant under the fuel-rich condition at high temperature and it acts as an excellent soot suppressant. Millikan also found that the critical equivalence ratio increases with increasing temperature. This fact can be explained by difference in the relative activation energies of oxidation as well as precursor formation. The activation energy of oxidation (290kJ/mol) is greater than the fuel pyrolysis (270kJ/mol) [21].

Furthermore, Fenimore et al. found that 10% collision of OH radicals with the soot molecules can abstract carbon [22]. In another study of soot burnout in flames with different oxygen partial pressures and at 1600-1850K, Neoh et al. [23,24] concluded 20% collision probability of OH radical to abstract carbon. OH is assumed to be the primary oxidant of soot particles or precursors, but sometimes when the OH concentration is low, especially at low temperature, O_2 becomes an active radical which is also not considered as a very good oxidant due to its stability as compared with the OH radical.

2.6.2 Ionization

Combustion flames are usually associated with the production of ions called chemi-ions which are also considered as the driving factor that might influence the soot formation and growth processes [25]. The characteristic of these ions changes drastically from non-sooting to sooting flames. Usually, this phenomenon has been investigated by application of electric field and observing macroscopic changes induced or extrapolation of ions produced in non-sooting flames to sooting flames [26]. A direct sampling experiment in sooting flame provided insight into a new ionization mechanism which was different from the conventional chemi-ionization.

The comparison of non-sooting and sooting acetylene and ethylene air flames clearly indicate the presence of smaller (12-300 amu) ions in non-sooting flames and bigger ions (>700 amu) in sooting flames [27].

These ions are subjected to an electrostatic force which is considered a primary driver inhibiting their coagulation [28]. Coagulation was inhibited by the presence of ionization additives, mainly alkali metals. The reason being charged particle will not coagulate thus inhibiting surface growth by coagulation. This, in turn, reduces the overall soot volume fraction [29].

Soot formation and growth in ionized flames can be controlled by applying an external electric field, which decreases the residence time of charged particles in the pyrolysis zone and accelerates them out quickly leading to smaller particles and less soot. This argument was further strengthened by applying a controlled electric field so that the residence time of the particles in the pyrolysis zone increases which leads to particle coagulation and more soot. In this study, the mass of soot deposited reduced to almost 10% of the original soot mass fraction without electric field [30].

2.6.3 Additives

The influence of additives on soot formation is manifold. It depends on the qualitative as well as quantitative aspects of the additive. Usually, inert diluents are an effective mean of reducing soot yield at a constant temperature. But dilution is usually accompanied by a reduction in the temperature which promotes soot formation. There is a trade-off between these two effects. Adding inert diluents (conc.>5%) has practically no influence on the critical sooting equivalence ratio [31]. Adding nitrogenous species, i.e., NH_3, NO and NO_2 aide in raising critical sooting C/O ratio and also reduces soot yield. Adding nitrogenous species tend to form unreactive HCN by abstracting carbon from the fuel. For each nitrogen atom bonding carbon in HCN, the mixture becomes leaner thus increasing critical sooting C/O ratio [32]. Sulpur compounds like H_2S and SO_2 are very effective in reducing soot as well as increasing the critical sooting equivalence ratio. Adding 1% to ethylene/air reduces the soot by almost 85% [33]. Adding H_2 or CO increases soot yield and decreases critical C/O ratio because these species are easily oxidized by oxygen forming CO_2 and H_2O, which makes the flame effectively fuel-rich thus increasing sooting. Adding hydrocarbons results in increasing the carbon content thus promoting soot [34].

Usually, non-metallic compounds have little effect on mitigating soot with Sulphur compounds being the most effective additives [33]. Metal additives are generally used as soot /smoke suppressant in commercial applications. Salooja concluded that manganese is the most effective of all the metal additives in reducing soot while barium, iron, nickel, cobalt, and copper have also shown potential to reduce soot in some applications. These additives act as a catalyst for promoting the oxidation/gasification of soot particles [35]. Another explanation for the same process

was given by Bartholome et al. who concluded that metal additives are effective in ionizing the soot particles, which in turn inhibit coagulation because of charge repulsion among the ions which results in their easy oxidation. Addecott et al. stated that the additives which are easily ionized can reduce the concentration of precursors by simple charge transfer as shown below.

$$C_nH_m^+ + M \leftrightarrow C_nH_m + M^+$$

The additives introduced at different points in the same flame may have different effects on the resultant soot formation processes as studied by Salooja [36]. He concluded that soot promotion was strongest when the wire coated with low ionization potential salts like Cesium and Potassium, was held at the tip of the primary zone. Soot was inhibited when the wire was placed at the base of the primary reaction zone. He explained these results based on the additives ability to produce electrons. When introduced at the tip, the positively charged soot particles were neutralized by these electrons which then become susceptible to coagulation thus becoming resistant to the oxidation later by the OH. When introduced at the base of the primary reaction zone, these electrons neutralize the flame ions which reduces the ionic nucleation of soot particles, thus inhibiting soot [36].

Cotton et al. [37] proposed that the alkane earth metal as well as Ba, SO_2 and NO reduces soot due to their ability to act as a catalyst for the equilibrium reaction,

$$H_2O \leftrightarrow H + OH$$

which can provide additional OH radicals for soot oxidation by the following reaction:

$$C_s + OH \rightarrow CO + \frac{1}{2}H_2$$

Feugier [38] with a 500ppm metal concentration in premixed ethylene-air flame found the ionic effects for alkali metals, i.e., Na, K, and Cs which tend to increase soot loading by the reverse reaction:

$$C_nH_m^+ + M \leftrightarrow C_nH_m + M^+$$

Alkaline earth, i.e., Ca, Sr, Ba, and Li provide OH radical as explained previously by Cotton et al. which helps in incipient soot oxidation.

Haynes [39] on the other hand found very different results with a 2ppm metal concentration in premixed ethylene-air flame. He concluded that both alkali earth and alkali metals suppressed soot although in rather different ways. The differences in Haynes et al. and Feugier was attributed to the different concentration of metals used.

2.7 Experimental Techniques

To understand fully the physics of particle formation and evolution during combustion, there is a need to carefully quantify their formation and growth during combustion which still has certain shortcomings. These shortcomings are generally attributed to the lack of accurate methods to quantify soot during its evolution in the combustion chamber. The simulation of soot inception and growth via nucleation of particles and later oxidation is very difficult to follow. These are some of the obstacles that need to be overcome to get a better understanding of all the processes involved in soot formation which can then be utilized in devising techniques to mitigate soot by suppressing either soot inception or growth.

There is a need to measure soot inception and growth by measuring particle size, morphology, and composition. Ex-situ methods have been employed previously to assert these properties of particles, but they occur at the expense of perturbing

combustion, i.e., thermophoretic sampling is used to measure soot volume fraction. To ascertain soot inception and initial growth, it is necessary to resolve the spatial and temporal evolution of particle size distribution in the range of 1-10nm. A thermocouple can be inserted into the combustion zone to collect soot. As the soot build up on thermocouple, the measured temperature changes which can be modeled to ascertain the rate of soot collection on the surface and in turn can give volume fraction of soot [40]. The particle collected can then be analyzed using a transmission electron microscope (TEM). The advantage is that no prior knowledge of particle density and refractive index is required. This technique has an inherent disadvantage of perturbing the flow and the exact temperature of the particular section is necessary to reduce the error.

To understand the soot inception and growth process, there is a need to analyze soot particle size distribution function along the reactor length which is done using Scanning Mobility Particle Sizer (SMPS). SMPS is able to detect newly incepted particles less than 10nm which is difficult to detect by optical techniques because the optical properties of newly incepted particles are unknown.

In situ measurements are very unique in a sense that they can provide information about particle inception and growth without perturbing the combustion chemistry. Using optical techniques require a firm understanding of the optical properties of particles beforehand. The optical method includes laser light incandescence (LII) and laser scattering and extinction techniques. LII is used because of its inherent simplicity and ease to resolve spatial and temporal signal [41]. The basic principle behind LII is that the particles are heated to sublimation temperature using laser light and the signal returned is approximately proportional

to the volume fraction. To determine the particle size (diameter) the LII signal is resolved with respect to time and the decay of the signal corresponds to the cooling rate of the soot particle. Then these decay curves can be compared with the theoretical curves to resolve size [42]. Uncertainties in this method may come from inaccurate flame temperature measurements while taking LII measurement because the cooling of particles is a strong function of combustion temperature.

While studying soot inception and growth, there is a need to identify species forming and evolving in each reaction stage leading up to soot formation. This is done using gas chromatography or mass spectrometry.

2.8 Motivation

The motivation of current research is driven by the detrimental impact of the current state-of-the-art combustion technologies on the environment in terms of soot and other pollutants emissions. This study aims at studying low-temperature soot in a micro-flow reactor with externally controlled temperature profile. Operating at lower temperature has benefits when it comes to fuel cell applications. This work aims to investigate the micro-flow reactor for conditions where soot can be avoided. The aim is to operate at a higher equivalence ratio for more syngas generation and at a temperature that will reduce soot formation.

2.8.1 Low Temperature Soot Studies

Generally, in the combustion community, it is widely accepted that increasing temperature decreases soot and vice versa. Milliken found that the cooler flame tends to form more soot than the hotter flame and decreases the critical sooting equivalence ratio [19]. In the sooting flame, there are two processes occurring simultaneously: the

pyrolysis rate of fuel forming precursors (i.e. acetylene), which can further lead to other precursors forming a benzene ring that polymerizes to form soot, and the rate of oxidation of these precursors by OH radical. Increasing the temperature increases both rates, but the oxidative rate increase overwhelms the pyrolysis rate increase, thus diminishing the tendency of the flame to soot [43]. This trend is verified by other investigators too who showed that the soot increases with increasing temperature in co-flow diffusion flames because there is no oxidative attack on the precursors [13].

Shock tubes, as well as flow reactors, have been employed previously to study the temperature dependence of soot formation and its oxidation. Recently Koki et al. [11] studied benzene pyrolysis and PM (particulate matter) formation using a meso-scale flow reactor. The effect of varying temperature and oxygen concentration on PM formation was studied. They concluded that less PM was formed at a lower temperature compared to a higher temperature as shown in Fig. 5.

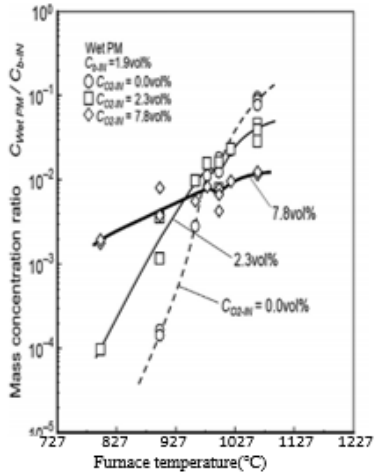

Figure 5: PM formation under various temperatures and oxygen concentration [11].

At low temperature (777-876℃) less PM formed without oxygen and it increases with oxygen addition. Under 876℃, oxygen coupled reactions [44] promote soot as indicated by Wang et al. [45]. At high temperature (>977℃) large PM formed

without oxygen, which decreases with oxygen because of the activation of oxidation reactions. This nature of temperature dependent oxidation was explained by Peter et al. [46] who suggested that at low temperature (<900℃), oxygen attacks the methyl group rather than the aromatic ring allowing soot formation. At higher temperatures (>977℃), oxygen attacks the ring directly thereby suppressing soot. Also, a higher temperature promotes the production of OH radicals, which is a good oxidizer. A similar trend was observed by Frenklach et al. [44].

On the other hand, Bikau et al. suggested that under low-temperature conditions, hydrocarbons formed by benzene pyrolysis are difficult to grow up to heavier PAHs, which are regarded as the precursors for soot formation, thus suppressing soot at low temperature [47]. Frenklach et al. [48] observed a bell-shaped trend for soot formation from 1027-1927℃. Soot suppression effects were found at temperatures around 1027℃. Wang et al. [45] concluded that increasing oxygen partial pressure slowed down the soot formation processes at a higher temperature (>1227℃) and has a negligible effect at a lower temperature (<1227℃) as indicated by Fig 6.

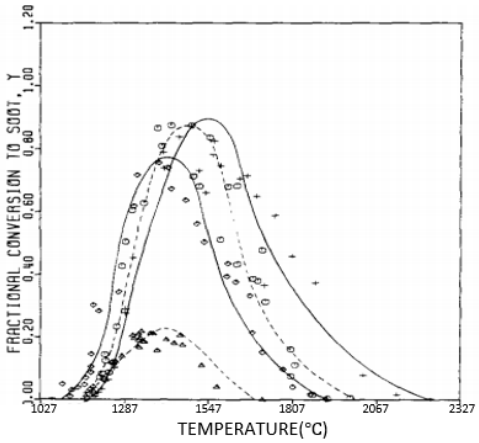

Comparison of soot yield at 2.5 msec after the onset of reflected shocks during oxidation of toluene. A: ○, C_7H_8=.3%, O_2=0.21%; B: △, C_7H_8=.3%, O_2=0.3%

Figure 6: Soot yield comparison [45].

Below 1527°C, increasing oxygen partial pressure increases soot yield because at lower temperatures the aromatic ring structure remains intact and increasing oxygen partial pressure aides in the condensation of PAH onto the soot particle thus increasing final soot yield [45]. Increasing oxygen partial pressure and temperature beyond 1527°C promotes the fragmentation processes in which the rate of fuel decomposing to smaller hydrocarbons is faster than the dehydrogenation and polymerization rate, thus decreasing soot yield. Feiyang et al. found for a diesel engine that the total soot yield reduced by an order of magnitude at 627°C compared to 727°C with 15% oxygen content in the constant volume combustion chamber [49].

Recently Maruta et al. [7] successfully demonstrated soot and PAH formation processes for methane and acetylene in a micro-flow reactor with a controlled temperature profile. The dependency of sooting limit on equivalence ratio and flow velocity (residence time) were identified. Also, the temperature dependence of soot precursors was obtained at long residence time and a temperature ranging from 327-727°C. It was observed that the soot precursors molar concentration increases from 327°C to 727°C as shown in Fig. 7.

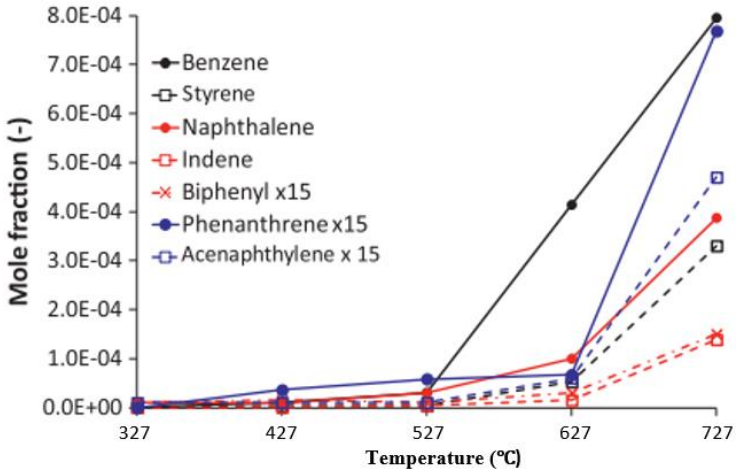

Figure 7: Temperature dependence of PAH mole fraction at a flow velocity of 2cm/s and at Φ=4 [7].

Milcarek et al. [8] studied the temperature dependence of soot formation for propane for an equivalence ratio 1-5.5 using a micro-flow reactor as a fuel reformer. They observed no soot in the temperature range 750-900℃ for equivalence ratios 1-5.5, while soot formation was observed at 950℃ and 1000℃ at equivalence ratios above 2.5. Moreover, the syngas concentration in the exhaust was a strong function of temperature. At an equivalence ratio of 3, increasing temperature from 750℃ to 900℃ increased the syngas concentration from 2.3mol% H_2 and 10.7mol% CO to 9.2mol% H_2 and 15.3mol% CO. Increasing temperature further to 950℃ and 1000℃ didn't change the syngas concentration much and soot generation occurs.

To date, limited work has investigated soot formation at low-temperatures in a micro-flow reactor. This work aims to investigate the micro-flow reactor for conditions where soot can be avoided. The aim is to operate at a higher equivalence ratio for more syngas generation and at a temperature that will reduce soot formation.

CHAPTER 3

EXPERIMENTAL SETUP

In this investigation, propane is used as a fuel. A gas chromatograph (GC) is being used to investigate soot precursor formation such as C_2H_2. A meso-scale reactor made up of a quartz tube with an inner diameter of 2.6mm is used as shown in Fig.1. For better visualization of soot luminosity and radiation, a hydrogen/air flat flame burner was sought to be used as an external heat source. However, due to limitations in the hydrogen flow rate, a resistive wire heater was used. The wire heater was wrapped around the reactor and the power input was controlled by an external power supply. The heater created a stationary temperature profile along the inside of the reactor referred to in this text as the wall temperature. The wall temperature is measured by an Inconel-sheathed K-type thermocouple with a 1mm diameter inserted from the exit of the reactor. The premixed propane/air mixture is sent to the flow reactor using mass flow controllers. The equivalence ratio was varied by fixing the total fuel and airflow rate and then varying each to get the proper equivalence ratio. The mixture entered the flow reactor at atmospheric conditions. When it passes through the tube where the resistive element was wrapped, the temperature rises and reaches the value needed to sustain combustion inside the reactor. The flame sooting characteristics were observed by varying the parameters as follows:

- Equivalence ratio, Φ : 1-13
- Total flow rate : 10sccm, 100sccm,10sccm propane/air & 90sccm N_2
- Temperature range : 800-1250℃

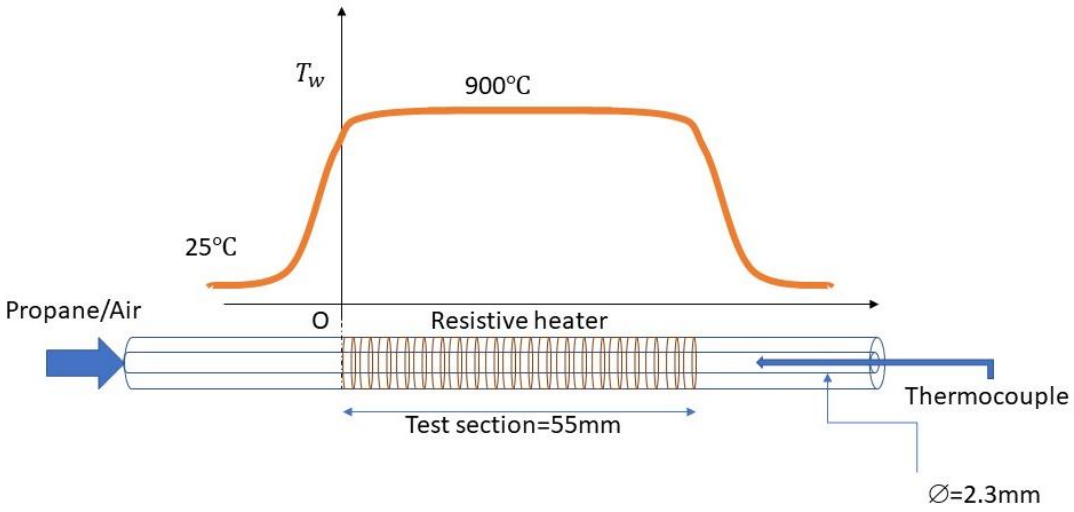

Figure 8: Micro flow reactor with a controlled temperature profile.

To ascertain the onset of soot formation, a digital camera (Nikon D850) is used to capture images of the reactor. The final syngas concentrations and the precursors concentration were collected at the end of the reactor and further investigated using a GC-2014 (Shimadzu) which can measure the syngas as well as hydrocarbons up to C_6.

This study is divided into two main sections;

1) Visual Soot analysis

   In the first section, the onset of yellow luminosity is used as an indicator of soot formation which is captured by using a camera. This study includes the parametric analysis with temperature, equivalence ratio and flow rates (residence time) as the controlling parameters to ascertain soot inception and growth with these parameters. These results will give an insight into the extent/limits to which we can go to generate as much syngas as possible without soot formation.

2) Precursors Species Formation

In the second part of the experiment, the Micro-combustion exhaust is investigated for the temperature range of 750℃ to 1250℃ at an equivalence ratio of 2.5 and mixture flow rate of 20sccm to ascertain that we are generating a comparable amount of syngas for non-sooting flame when compared with the sooting flame.

3.1 Gas Chromatography

The final syngas concentrations and the precursors concentration were collected at the end of reactor and further investigated using a GC (Shimadzu) "2014 Fast Refinery Gas Analyzer" fitted with two TCDs (thermal conductivity detectors) and one FID (flame ionization detector) which can measure the syngas as well as hydrocarbons up to C_6. The C_6+ components are backflushed as a single peak. Another GC used is the GC-2014 CAP FID, which can detect up to C_{20} hydrocarbons.

Gas chromatography is a technique intrinsically used for separation and detection of chemical compounds (organic & inorganic) in a mixture. The sample gas is dissolved in a mobile phase which is then forced through an immiscible phase. Owing to the different solubility of sample gas components, the component which is not very soluble in the stationary phase will take a shorter time to travel through the stationary phase than the component which is very soluble in stationary phase and not very soluble in the mobile phase. Hence the components of the sample gas mixture get separated from each other as they travel through the stationary phase.

With a gas chromatograph, chemical composition of mixture gases coming out of the reactor can be determined. Different techniques are used to determine different kind of gas components. Some of them are detailed below.

3.1.1 Thermal Conductivity Detector(TCD)

TCD is a non-destructive technique used to analyze inorganic gases and small hydrocarbon molecules up to C_2. The working principle of a TCD is that it compares the conductivity of the carrier gas and the sample gas. The detector consists of electrically heated wires whose temperature changes with the thermal conductivity of the gas around it. This changes the electric resistance of the heated wire and is measured by a Wheatstone bridge. One TCD measures H_2 in the experiments and the other TCD measures CO, CO_2, O_2, and hydrocarbons up to C_2. C6+ components are backflushed as a single peak. The valve timing allows the hydrocarbons C_3-C_5 to be separated and detected by the FID.

3.1.2 Flame Ionization Detector(FID)

A flame ionization detector (FID) is a component of a GC that detects organic compounds by measuring the amount of carbon in the sample. It is a destructive detector. The principle of operation is based on the detection of ions formed during the combustion of organic hydrocarbons in a hydrogen flame. The ions concentration is proportional to the concentration of organic species in the gas stream. These ions are collected on the electrodes which measure the current from these ions. Only 1 in 10^5 carbon atoms produce an ion in the flame and the total amount of ions collected (current) is directly proportional to the amount of carbon in the sample.

3.1.3 GC Calibration

A GC can easily separate compounds, but it cannot quantify them by itself. A gas chromatograph usually needs to be calibrated with a calibration mixture of known concentration before it can be used to quantify and identify a gas mixture composition. By running some calibration standards with known concentration, the area under the curve can be related to the concentration of that component.

3.2 Quartz Reactor

A 2.3mm inner diameter and 6.3 mm outer diameter quartz tube is used as a reactor. The length of the tube is 0.15 meters. The flow is introduced inside the reactor with the help of flow meters to control the equivalence ratio of the mixture as well as the flow velocity (residence time) accordingly. The reactor is maintained at the required temperature with the help of an external resistive heater. The temperature of the reactor can be changed by changing the power input to the heater. The reaction residence time can be changed by changing total gas flow rates.

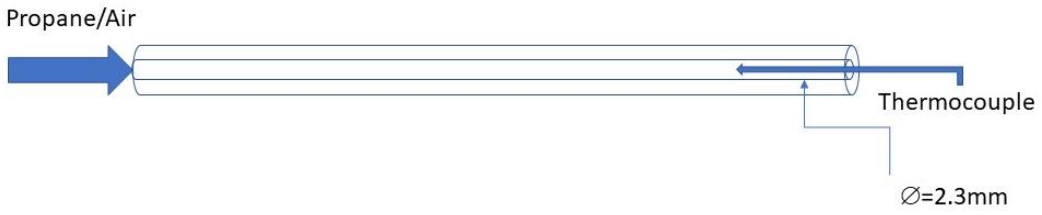

Figure 9: Quartz reactor.

Two mass flow controllers control the flow rates of propane and air. These gases are mixed before they enter the quartz reactor. A flame arrestor is also connected upstream of the reactor feed line for safety.

3.2.1 Temperature Control

The temperature of the reactor was crucial for these experiments to have a controlled wall temperature profile on the inside of the quartz reactor. Maruta et al.[8] used a hydrogen flat flame burner to control the temperature profile of the reactor which requires a very high flow rate of hydrogen (6000-15000sccm). Initially, we tried to replicate the same setup with the hydrogen burner, but the flow rate we can achieve was not sufficient to get the reactor inside walls up to the temperature that we intended to use in our experiment. We used a hydrogen generator, the maximum capacity of which was around 600sccm and with this flow rate, the maximum inside wall temperature that we achieved was on the order of 800°C. The heating source was changed to the classical resistive wire heater. The wire heater was wrapped around the reactor as shown in the Fig.7 and the power input was controlled by an external power supply. The inside temperature of the reactor was measured by a K-type thermocouple with a diameter of 1mm. The temperature from the thermocouple is read into the LabVIEW using National Instruments data acquisition card (NI-DAQ).

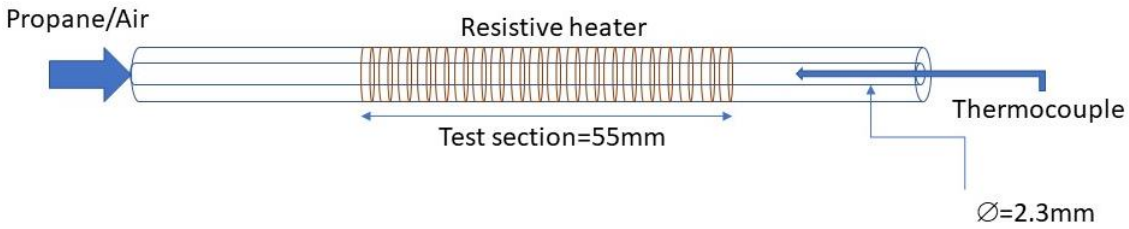

Figure 10: Quartz reactor with temperature control.

3.2.2 Controlling the Equivalence Ratio

The equivalence ratio is defined as

$$\Phi = \frac{\left(\frac{m_f}{m_a}\right)_{actual}}{\left(\frac{m_f}{m_a}\right)_{stoic}}$$

The overall stoichiometric reaction can be written as

$$C_nH_m + \left(n + \frac{m}{4}\right)(O_2 + 3.76N_2) \rightarrow nCo_2 + \frac{m}{2}H_20 + 3.76\left(n + \frac{m}{4}\right)N_2$$

Where for propane n=3 and m=8

Then the equation becomes

$$C_3H_8 + \left(3 + \frac{8}{4}\right)(O_2 + 3.76N_2) \rightarrow 3CO_2 + \frac{8}{2}H_20 + 3.76\left(3 + \frac{8}{4}\right)N_2$$

And, stoichiometric fuel/air mass ratio is

$$\left(\frac{fuel}{air}\right)_{stoic} = \left(\frac{m_f}{m_a}\right)_{stoic} = \frac{3 * 12 + 8 * 1}{\left(3 + \frac{8}{4}\right)(32 + 3.76 * 28)} = .007284\frac{12.3 + 8}{3 + \frac{8}{4}} = .0641$$

The flow rates of fuel and air can be defined as;

F_f= Propane flow rate in sccm and F_a= Air flow rate in sccm

Now, if its desired that the total flow rate to be=x, then;

$$F_f + F_a = x$$

And

$$\Phi = \frac{\left(\frac{m_f}{m_a}\right)_{actual}}{\left(\frac{m_f}{m_a}\right)_{stoic}} = \frac{\left(F_f * Molar\ mass\ of\ propane\right)}{(F_a * Molar\ mass\ of\ air)} = \frac{F_f * 44.1}{F_a * 28.97}$$
$$\left(\frac{mf}{ma}\right)_{stoic}$$

For some specific Φ and flow rate x, we have two equations and two unknowns, so we can easily find the mass flow rate of propane as well as air. Below is the sample Table for the total flow rate of 10sccm.

Table 1: Controlling the equivalence ratio for a total flow rate of 10sccm

Propane Fuel	n	m	Φ	Ff/Fa	Ff+Fa	Fa	Ff
No of atoms	3	8	1	0.04211	10	9.595916	0.404084
Stoic. Ratio	0.064103		1.5	0.063165	10	9.405878	0.594122
Fuel Molar Mass(g/mol)	44.1		2	0.08422	10	9.22322	0.77678
Air Molar Mass(g/mol)	28.97		2.5	0.105275	10	9.047522	0.952478
Molar Ratio	1.522264		3	0.12633	10	8.878393	1.121607
Total Flow Rate(sccm)	10		3.5	0.147385	10	8.71547	1.28453
			4	0.16844	10	8.55842	1.44158
			4.5	0.189495	10	8.406929	1.593071
			5	0.21055	10	8.260708	1.739292

3.2.3 Mass flow Controllers

The mass flow controllers from Brooks Instruments are used to control the mass flow of air, propane, and nitrogen inside the reactor. They were originally calibrated for nitrogen. A correction factor was multiplied by the calibration depending on the gas used, i.e., the correction factor for air and nitrogen is 1 and it is 0.35 in case of propane.

After applying the relevant correction factor, they were calibrated using a bubble meter. Using the bubble meter (bubble-o-meter), the volumetric flow rate can

be obtained by keeping track of the time it takes for a soap bubble to traverse across a known volume at a given flow rate. A calibration curve was obtained for each of the flow meters which was then inserted into the LabVIEW program to account for the adjusted flow rate. A sample calibration chart looks like this;

Table 2: Mass flow controllers calibration with a bubble-o-meter

ORIGINAL					
FLOW RATE(SCCM)	Distance	Time(s)	Time(min)	Measured flow rate	Error (%)
10	20	112	1.866666667	10.71429	6.666667
50	60	69	1.15	52.17391	4.166667
100	80	44	0.733333333	109.0909	8.333333
150	80	30	0.5	160	6.25
200	80	22	0.366666667	218.1818	8.333333
CALIBRATED					
10	10	60	1	10	0
50	20	23	0.383333333	52.17391	4.166667
100	80	46	0.766666667	104.3478	4.166667
150	80	32	0.533333333	150	0
200	80	23	0.383333333	208.6957	4.166667

For the initial run, the total flow rate of propane and air was 100sccm. The flow controller of 100sccm maximum flow rate was used for propane and 200sccm was used for air. The calibration curve obtained for air (200sccm) using a linear fit was;

$$x = \frac{y + 1.7211}{1.1029}$$

where x corresponds to the original flow rate and y to the adjusted flow rate.

Similarly, for propane (100sccm), the curve obtained was;

$$x = \frac{y - .1859}{1.104}$$

For a total flow rate of 10sccm, the flow controller of 30sccm was used for air and 10sccm was used for propane. Calibration curve obtained for air (30sccm) using a linear fit was;

$$x = \frac{y + .1875}{1.0795}$$

where x corresponds to the original flow rate and y to the adjusted flow rate.

Similarly, for propane (10sccm), the curve obtained was;

$$x = \frac{y - .0286}{1.0368}$$

For the third run, nitrogen was used as a diluent with the 10sccm propane/air with a combined flow rate of 100sccm, nitrogen flow rate being 90sccm. The flowmeter for nitrogen was calibrated again. Since nitrogen has the same correction factor as air, its calibration curve was similar to the one obtained in case of air with a 200sccm flow meter.

3.3 Methodology

The reactor was mounted with the resistive heating element wrapped around the tube. A thermocouple was inserted from the exit of the tube, touching the wall of the reactor. The power input to the reactor was controlled by the power supply. The required temperature was measured with a thermocouple at a specific power input to the reactor. The mass flow controllers were then turned on at a specific equivalence

ratio and the flow was allowed to stabilize inside the reactor to obtain sustained combustion.

3.3.1 Visual Soot analysis

To ascertain if there is soot at a certain equivalence ratio, pictures were taken before and after combustion and deposition of carbon particles was considered as an indication of soot generation at a specific equivalence ratio. A sample reactor before and after combustion with soot is shown in Fig. 11.

Figure 11 Reactor before(A) and after (B) combustion at a critical sooting equivalence ratio.

The critical sooting equivalence ratios were obtained for a temperature range of 800-1250°C with a 50°C interval. The critical sooting equivalence ratios were obtained for a total flow rate of 10sccm and 100sccm for propane/air mixture. Also, the critical ratios were obtained for a total flow rate of 100sccm with 10sccm of propane/air and 90sccm of nitrogen. The flow rate of 10 and 100sccm was chosen to see the effect of the residence time as well as the combustion temperature on the critical sooting equivalence ratio. The nitrogen dilution was investigated to obtain insight into the effect of inert gas dilution on the temperature and the critical sooting equivalence ratio.

3.3.2 Reactor Temperature Profile

After getting the critical sooting equivalence ratios, the temperature profile of the reactor was obtained using a thermocouple sweep. The wall temperature was fixed (e.g., 800 °C) in the middle of the reactor. The setup was run at the critical sooting

equivalence ratio and the thermocouple was swept across the reactor with a 50°C temperature interval and the distance was obtained at each of these intervals. The total reactor length was 55mm.

Two temperature profiles were obtained. One without combustion at a specified wall temperature and one with combustion at the same wall temperature. A sample temperature profile at Tw=800°C is shown in Fig. 12.

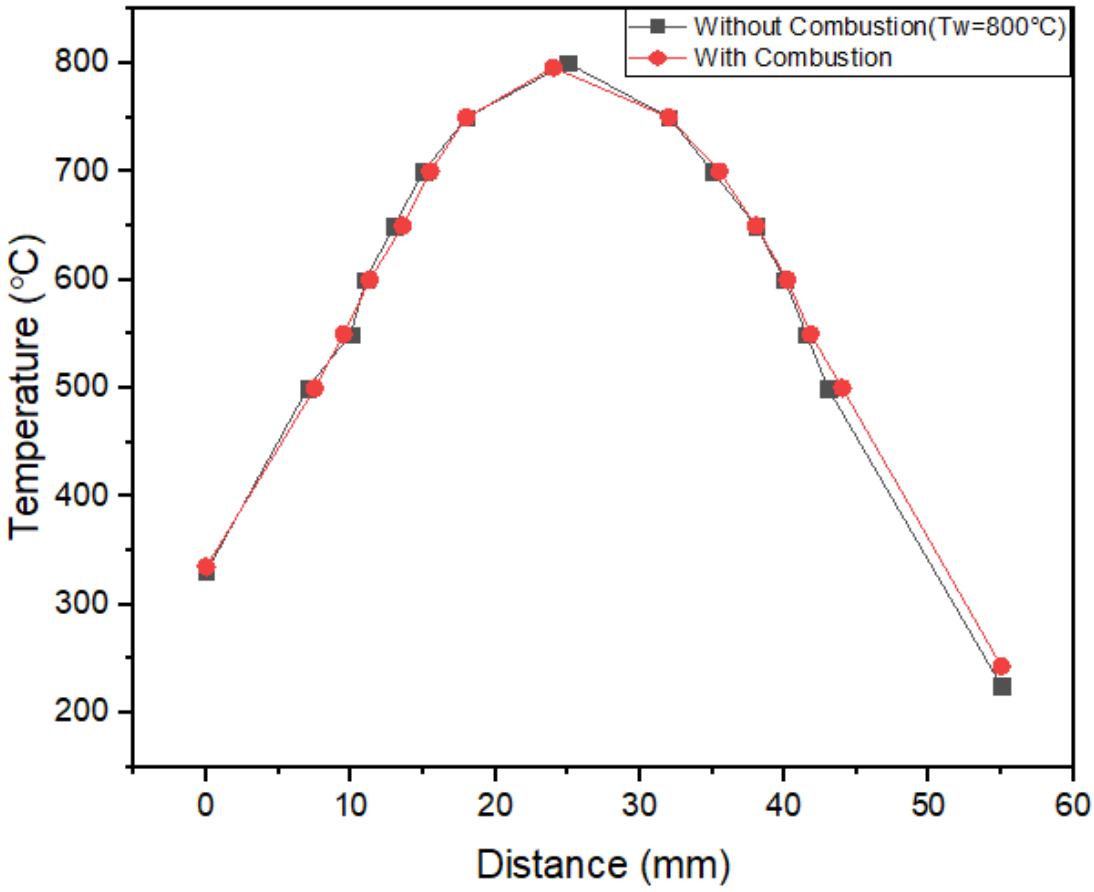

Figure 12 Reactor temperature profile with and without combustion at 800°C.

CHAPTER 4

RESULTS

The results section is divided into two sections. The first section deals with finding the critical sooting equivalence ratio through visual soot analysis and the second section deals with the temperature profiles inside the reactor using the temperature sweep with a thermocouple before and after combustion at the critical sooting equivalence ratios. The third section includes the GC results at critical sooting Φ and just before the critical sooting Φ to ascertain the mole fraction of the precursors as well as the gas composition.

4.1 The Critical Sooting Equivalence Ratio

The critical sooting equivalence ratios were obtained for a temperature ranging from 800°C to 1250°C and for a flow rate of 10sccm and 100sccm for a propane/air mixture. Nitrogen dilution was used to control the temperature for 10sccm propane/air case by adding 90sccm nitrogen.

4.1.1 Flow Rate of 10sccm

The total flow rate was fixed to 10sccm while the propane/air flow was adjusted with the help of flow meters to change the equivalence ratio. From 800-950°C, no soot was observed even at an equivalence ratio of 13. Soot started appearing at around Φ=2.5 at 1000°C. Increasing temperature beyond 1000°C resulted in a slight increase in the critical Φ and at 1050°C, critical Φ was around 3.2. The critical sooting Φ equals 3.7 at 1100°C. Further increasing the temperature beyond 1100°C decreased the critical Φ to 2.2 at 1150°C and 2.3 at 1200°C. Figure 13 shows all the data points

taken to ascertain the critical sooting equivalence ratio, where dark points show regions where soot was observed.

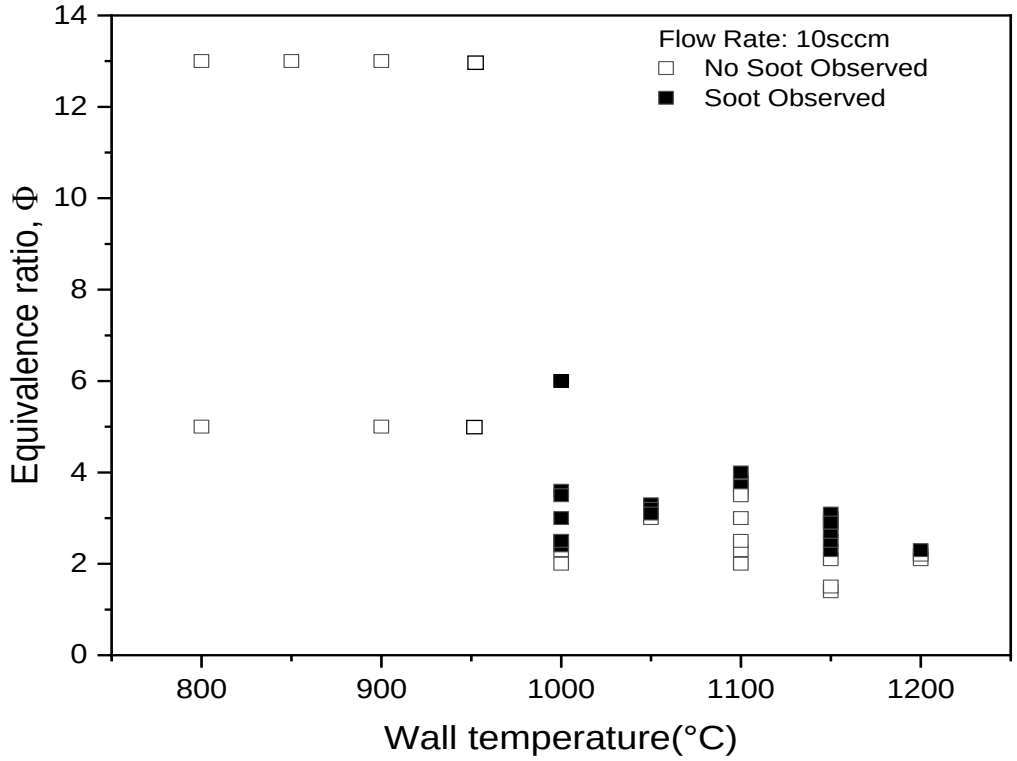

Figure 13: Critical sooting equivalence ratios vs temperature at a flow rate of 10sccm.

The trend lines give a clear indication of the temperature dependence of soot formation, which decreases drastically at temperatures below 1000°C and increases slightly from 1000°C to 1100°C where it hits the peak and drops down below to 2.2 around temperatures of 1150-1200°C. This trend is summarized in Figure 14.

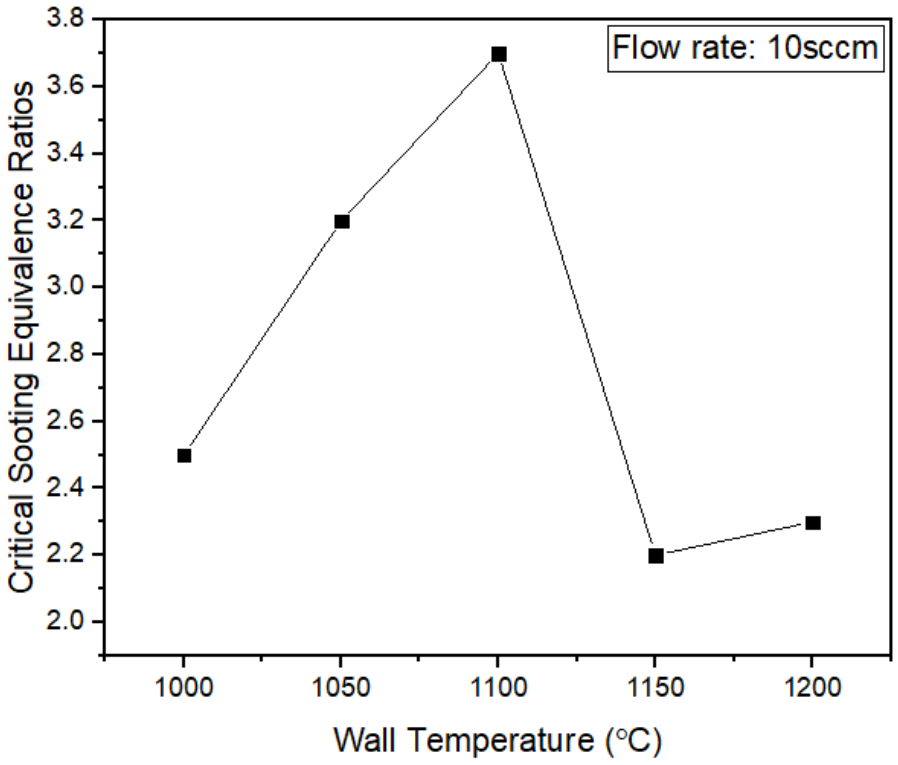

Figure 14: Trend line for the critical sooting equivalence ratios vs temperature at a total flow rate of 10sccm.

4.1.2 Flow Rate of 100sccm

To investigate shorter residence times and possibly higher local reaction temperatures, a total flow rate of 100sccm was investigated. The total flow rate was fixed to 100sccm while the propane/air flow was adjusted with the help of flow meters to change the equivalence ratio. From 800-950°C, no soot was observed even at an equivalence ratio of 13. Higher equivalence ratios up to 100 did not result in soot formation at these temperatures. Soot started appearing at around Φ=1.35 at 1000°C. Increasing temperature beyond 1000°C resulted in an increase in the critical Φ and at 1050, critical Φ was around 1.4. The critical sooting Φ equals 1.6 at 1100°C. Further increasing the temperature beyond 1100°C decreased the critical Φ to 1.5 at 1150°C

and 1.4 at 1200°C. Increasing temperature further decreases the critical Φ to 1.3 at 1250°C. The results are summarized in Fig. 15 and Fig. 16.

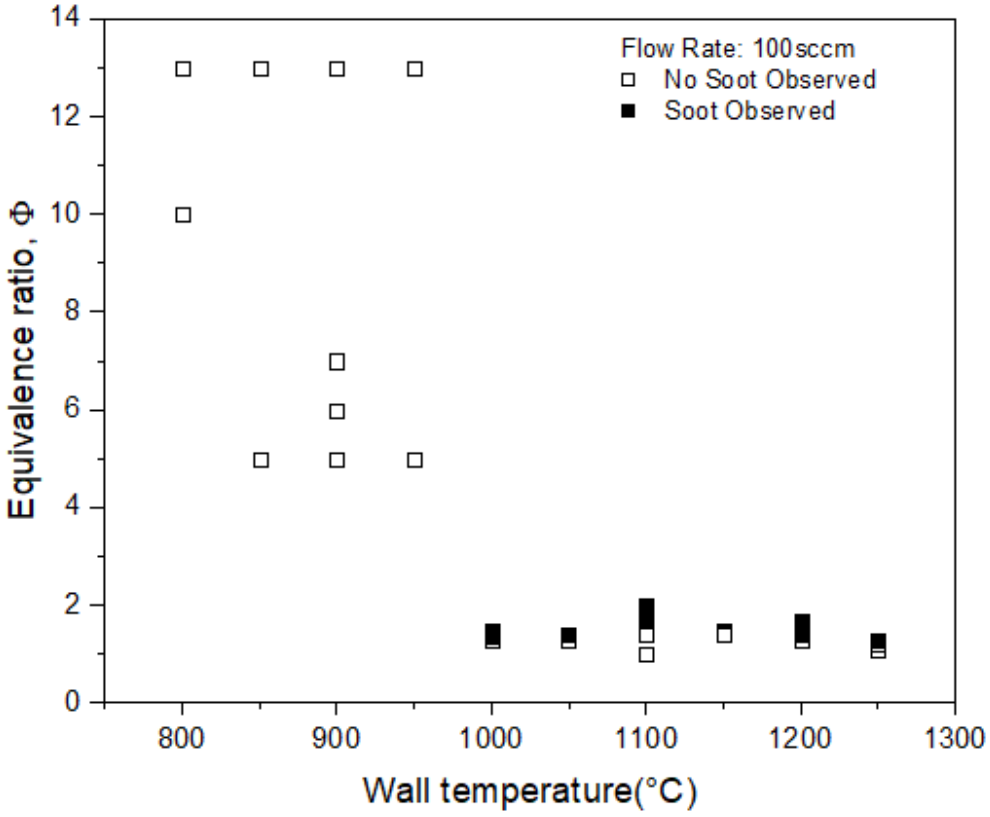

Figure 15: Critical sooting equivalence ratios vs temperature at a flow rate of 100sccm.

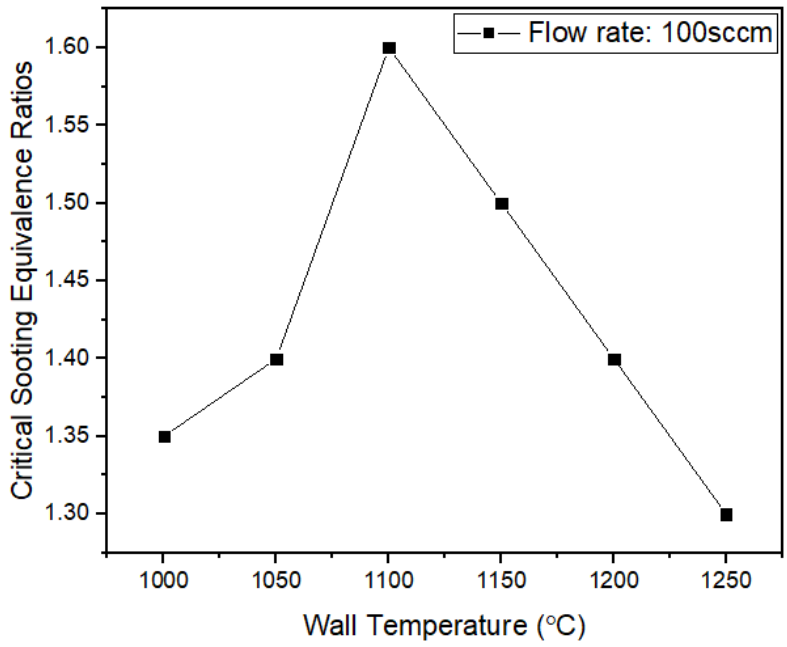

Figure 16: Trend line for the critical sooting equivalence ratios vs temperature at a total flow rate of 100sccm.

4.1.3 Flow rate of 100sccm (10sccm propane/air and 90sccm nitrogen)

Nitrogen was added as a diluent to reduce the local flame temperature, which could be higher than the wall temperature. Similar to the previous two runs, no soot was observed from 800-950°C at Φ as high as 13.

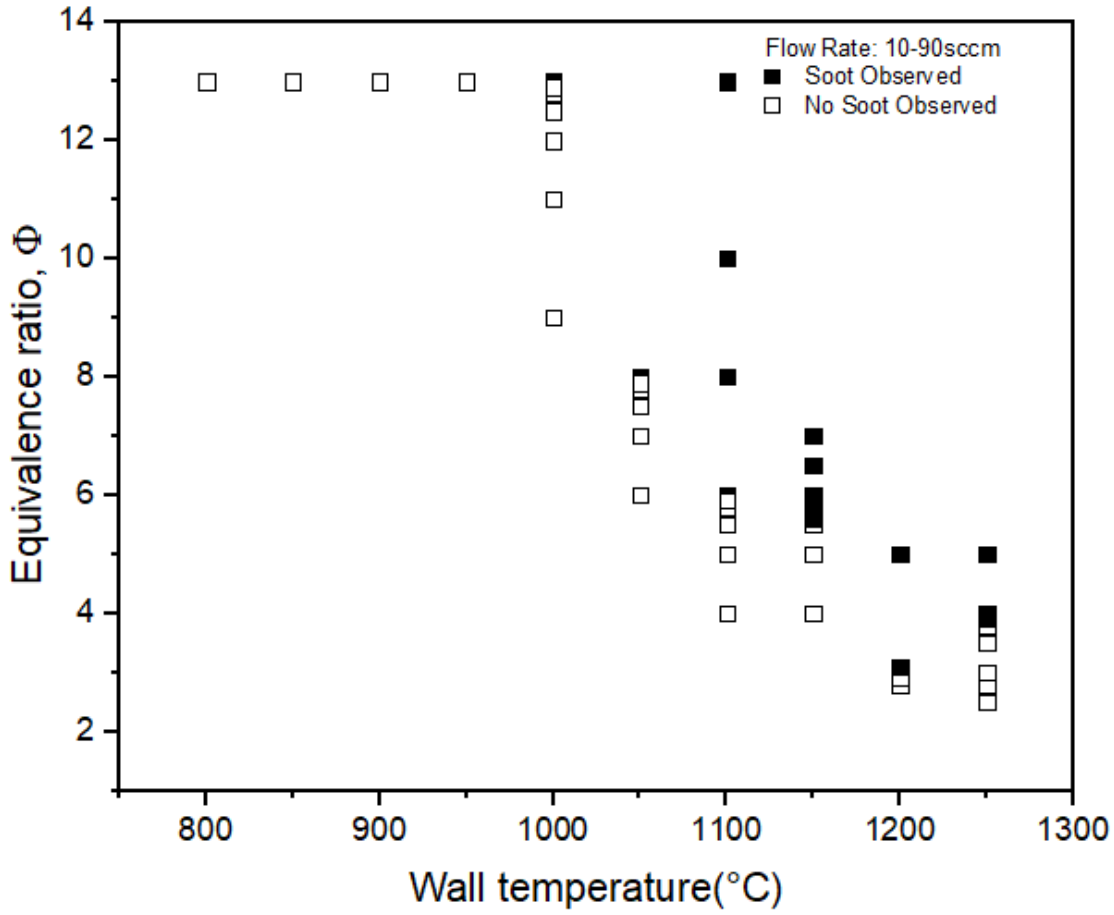

Figure 17: Critical sooting equivalence ratios vs temperature at a flow rate of 10sccm(10sccm(propane/air) + 90sccm N_2).

Soot started appearing at Φ=13 at 1000°C. Unlike previous results, increasing temperature further decreases the critical sooting equivalence ratio to 8 at 1050°C, 6 at 1100°C, 5.6 at 1150°C, 3.1 at 1200°C and 3.9 at 1250°C. The results are summarized in Fig.16.

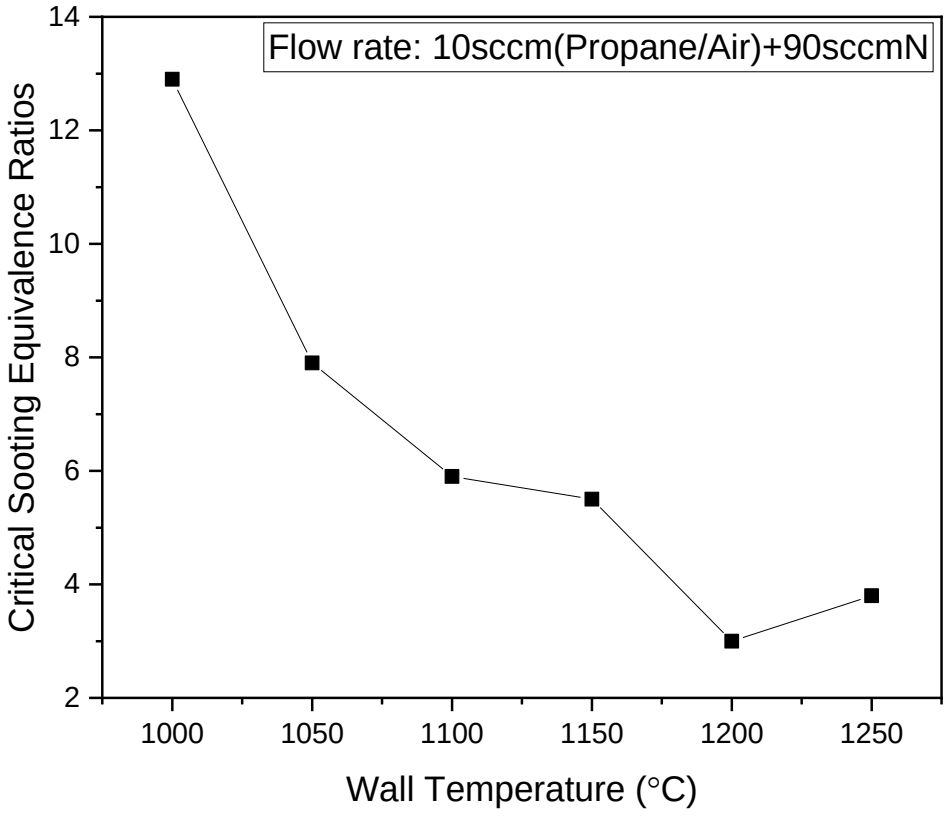

Figure 18: Trend line for the critical sooting equivalence ratios vs temperature at a total flow rate of 100sccm(10sccm(propane/air) + 90sccm N_2).

Figure 19 shows the critical sooting equivalence ratio trend line for all the flow rates to give an estimate of the difference in the critical sooting equivalence ratio variation with temperature. The main result is that at low temperature (<1000°C), soot formation is actually reduced. Thus soot formation can be reduced by increasing the temperature at higher temperature or by lower the temperature below a certain threshold temperature, 1000°C. It can be seen that the nitrogen dilution has a marked difference than the rest of the two cases. As nitrogen dilution is expected to lower the local flame temperature, the critical soot equivalence ratio appears to be much higher than observed at other conditions. The wall temperature and reaction temperature in the micro flow reactor with a controlled temperature profile is known to be tightly coupled. However, the addition of nitrogen may effect that temperature, which will be

investigated further in the next section. Furthermore, nitrogen may inhibit the formation of the initial benzene rings due to reduced residence time.

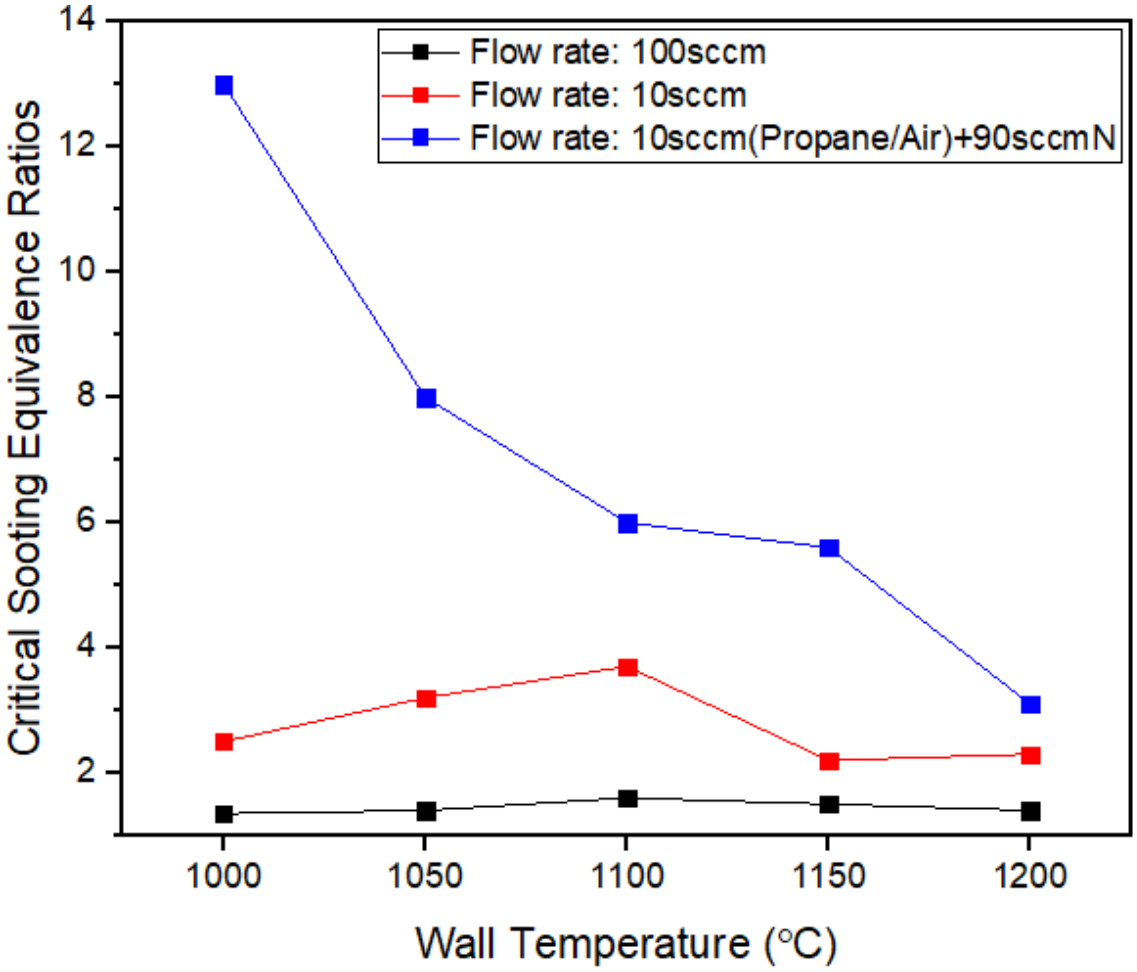

Figure 19: Comparison of the critical sooting equivalence ratios vs temperature at different flow rates.

Figure 20 shows the critical sooting equivalence ratios vs. the actual reactor wall temperature during combustion. It can be seen that the 100sccm case has a very marked difference between the combustion wall temperature with and without combustion (as high as 150°C in case of 1100°C wall temperature). That's why it has very low critical sooting equivalence ratio because higher temperatures beyond 1100°C aid in pyrolysis of propane thus producing more acetylene and subsequent soot formation. The profiles are not very different for the 10sccm case. In the case of

nitrogen dilution, the combustion wall temperature is actually lower than the actual wall temperature because dilution helps in reducing the reaction temperature. As shown, when the actual wall temperature is accounted for, the results for critical sooting equivalence ratio are actually more comparable than was suggested by Figure 19. If the actual reaction temperatures could be measured accurately, then these curves may align even more.

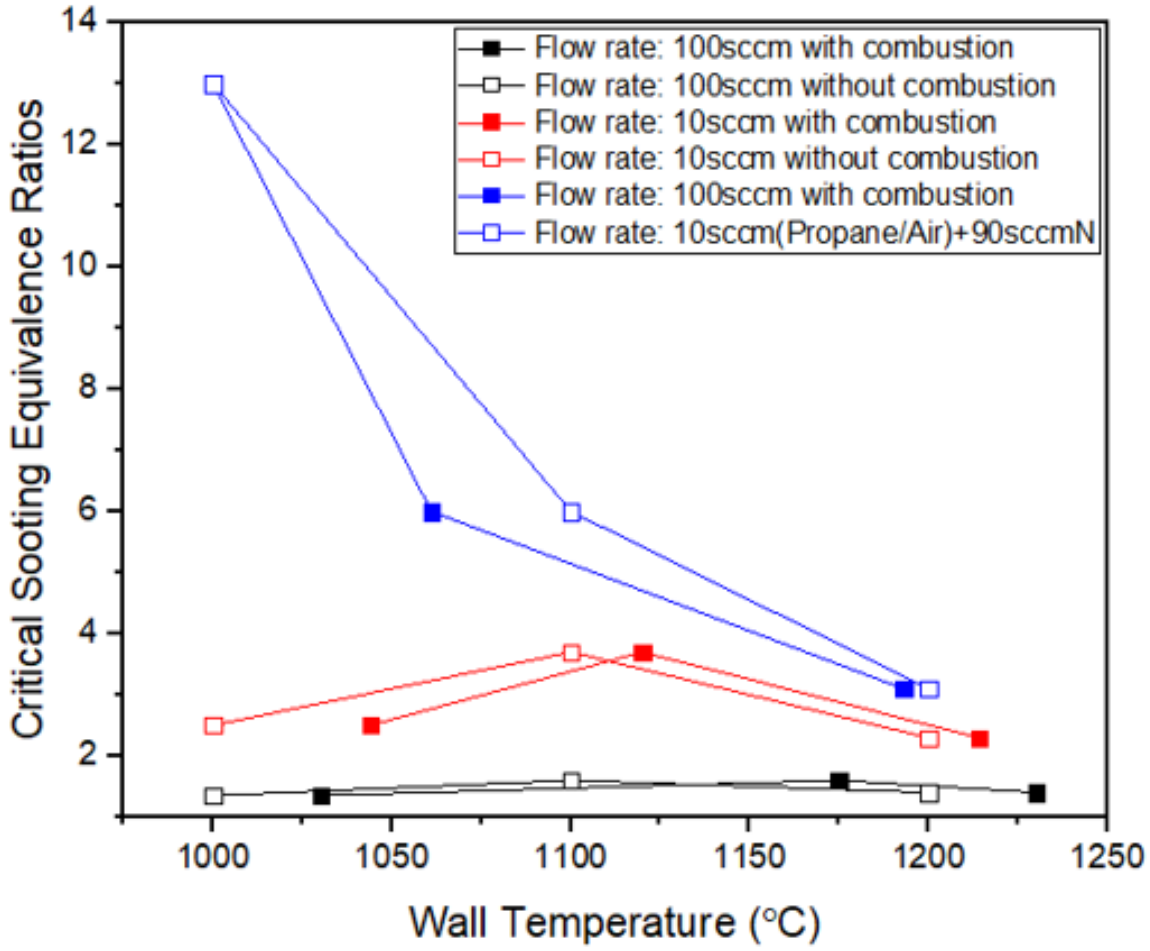

Figure 20: Comparison of the critical sooting equivalence ratios vs wall temperature with and without combustion.

4.2 Reactor Temperature Profile

The reactor temperature profile was obtained as explained earlier. The profiles were taken for 10sccm, 100sccm and for the nitrogen dilution case.

4.2.1 10sccm (Propane/air)

The results of the reactor wall temperature with and without combustion are shown in Figure 20. The temperature profiles with and without combustion are not very different in the case of 10sccm, because at this low flow rate the wall temperature inside the reactor was tightly coupled as shown in Fig. 20. The difference between the temperature with and without combustion was within a tolerance of ±10°C. At 800°C, the combustion wall temperature is slightly less than the wall temperature without combustion upstream of the maximum temperature zone. It becomes coincident with the wall temperature at the point of maximum wall temperature and even exceeds the wall temperature a little further downstream. It has a quite similar trend at 1200°C but the increase in the combustion wall temperature is a little more significant than the former case. This might be due to a higher combustion temperature achieved at 1200°C. The same trend follows for the whole temperature range of interest as shown in Fig. 21.

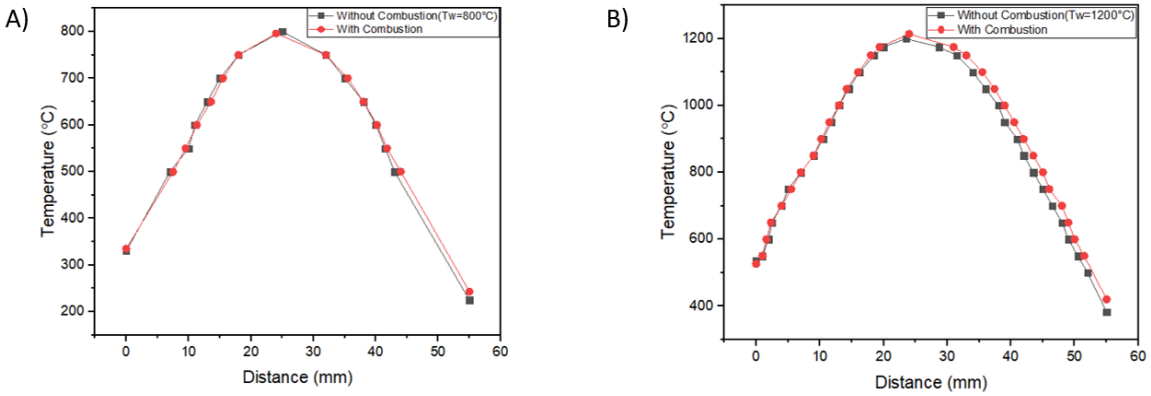

Figure 21: Reactor temperature profiles at A)800°C and B)1200°C with and without combustion at 10sccm.

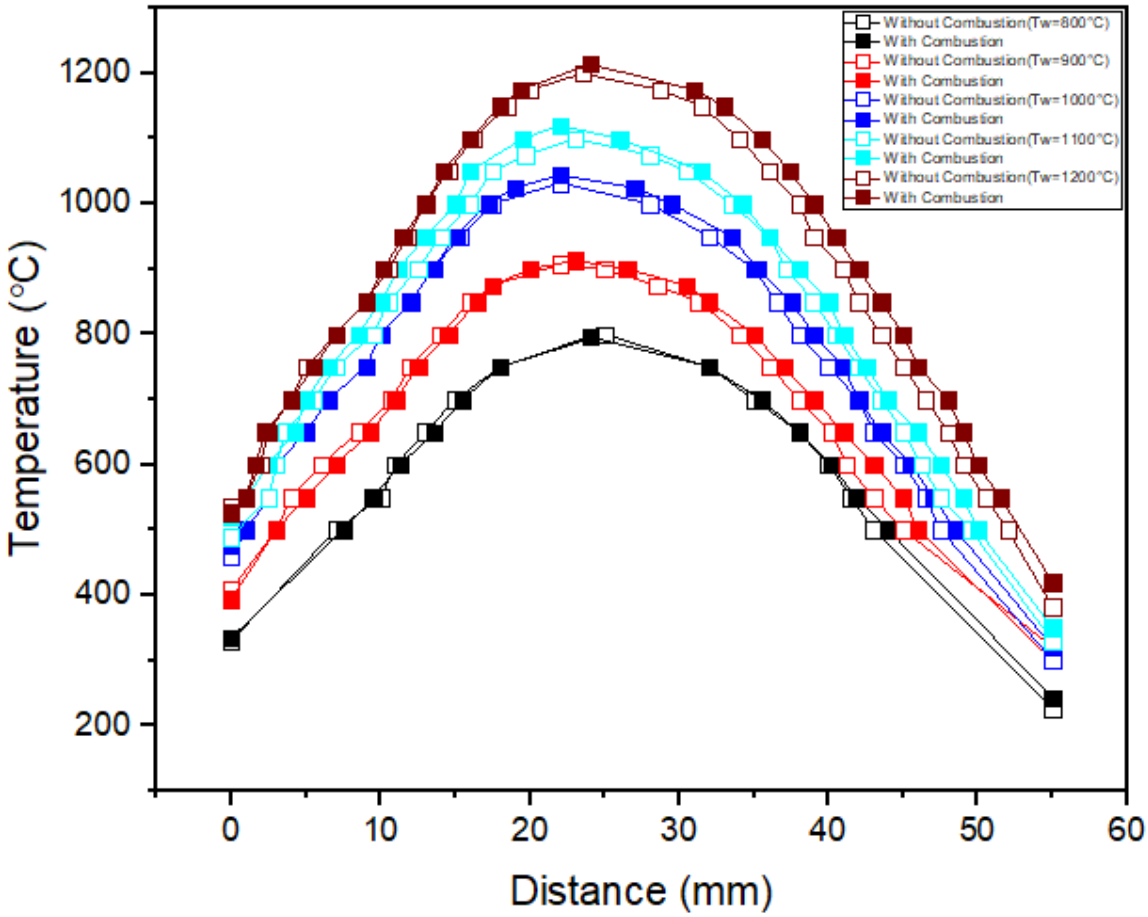

Figure 22: Reactor temperature profiles across the whole temperature's regime of interest at 10sccm.

4.2.2 100sccm (Propane/air)

The reactor temperature profile is quite different in case of a total flow rate of 100sccm, because of higher total flow rate. The higher flow rate has shifted the combustion temperature profile further downstream and it is significantly lower than the wall temperature profile for 800°C and 900°C until the middle of the reactor, where it starts to increases because the flame location was shifted downstream due to lower residence time. At higher wall temperatures, the wall temperature with combustion occurring increases beyond the wall temperature right at the upstream location, as shown in Fig. 23.

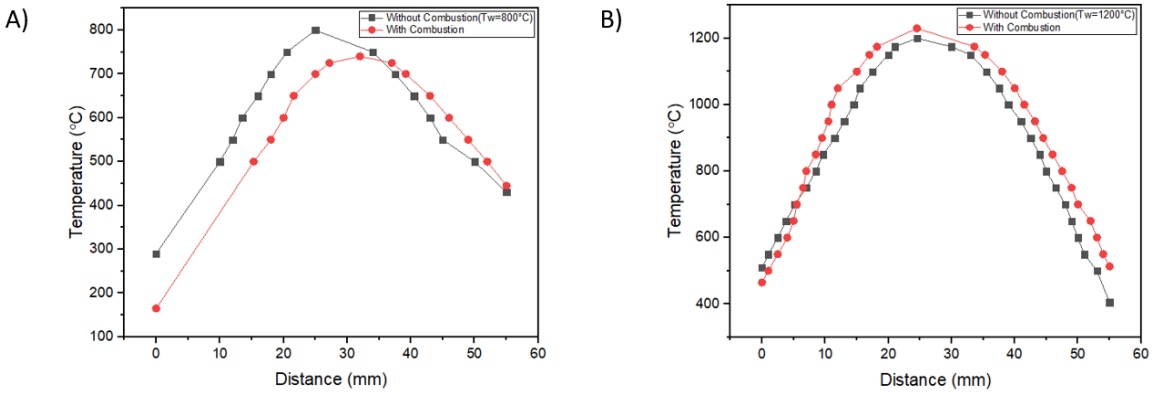

Figure 24: Reactor temperature profiles at A)800 °C and B)1200 °C with and without combustion at 100sccm.

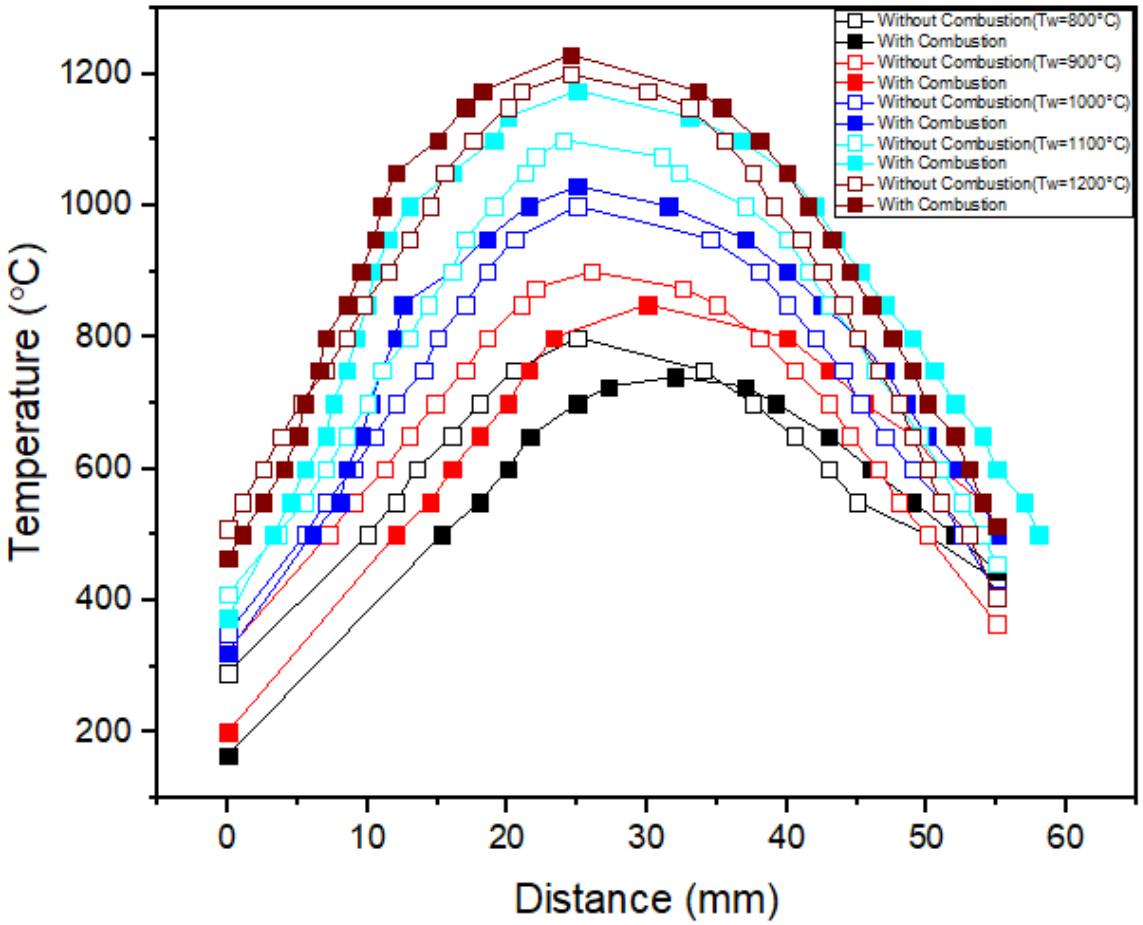

Figure 23: Reactor temperature profiles across the whole temperature's regime of interest at 100sccm.

4.2.3 100sccm (10sccm propane/air and 90sccm nitrogen)

Similarly, the temperature profiles with nitrogen dilution have the temperature profiles (Fig.25) which are similar to the one with a 100sccm total flow rate of propane/air at 800°C. Reduction in the residence time results in a shift in the temperature profile as occurred in the 100sccm case. Increasing temperature appears to shift the flame location further upstream and the flame is located approximately in the middle of the reactor as summarised in Fig.26. The combustion wall temperatures are less than the temperatures observed with 100sccm total flow rate because nitrogen dilution helps in reducing the combustion temperature inside the reactor.

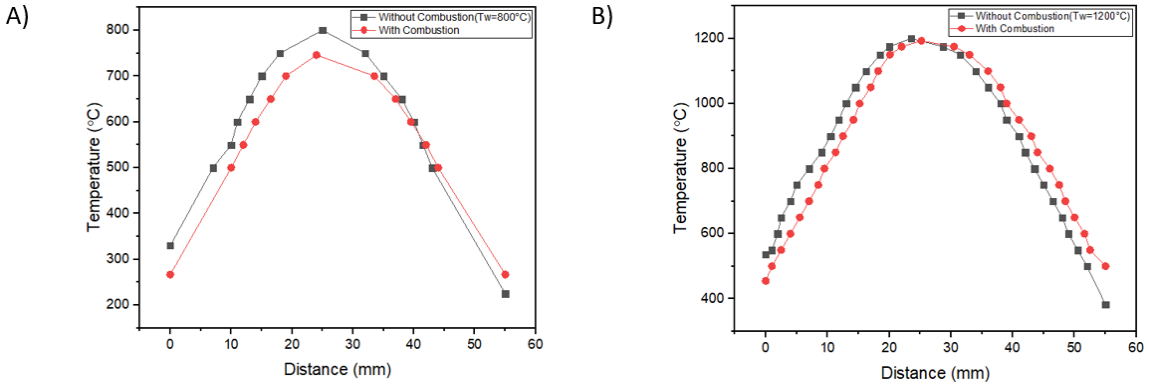

Figure 25: Reactor temperature profiles at A)800 °C and B)1200 °C with and without combustion at 100sccm (10sccm propane/air and 90sccm N_2).

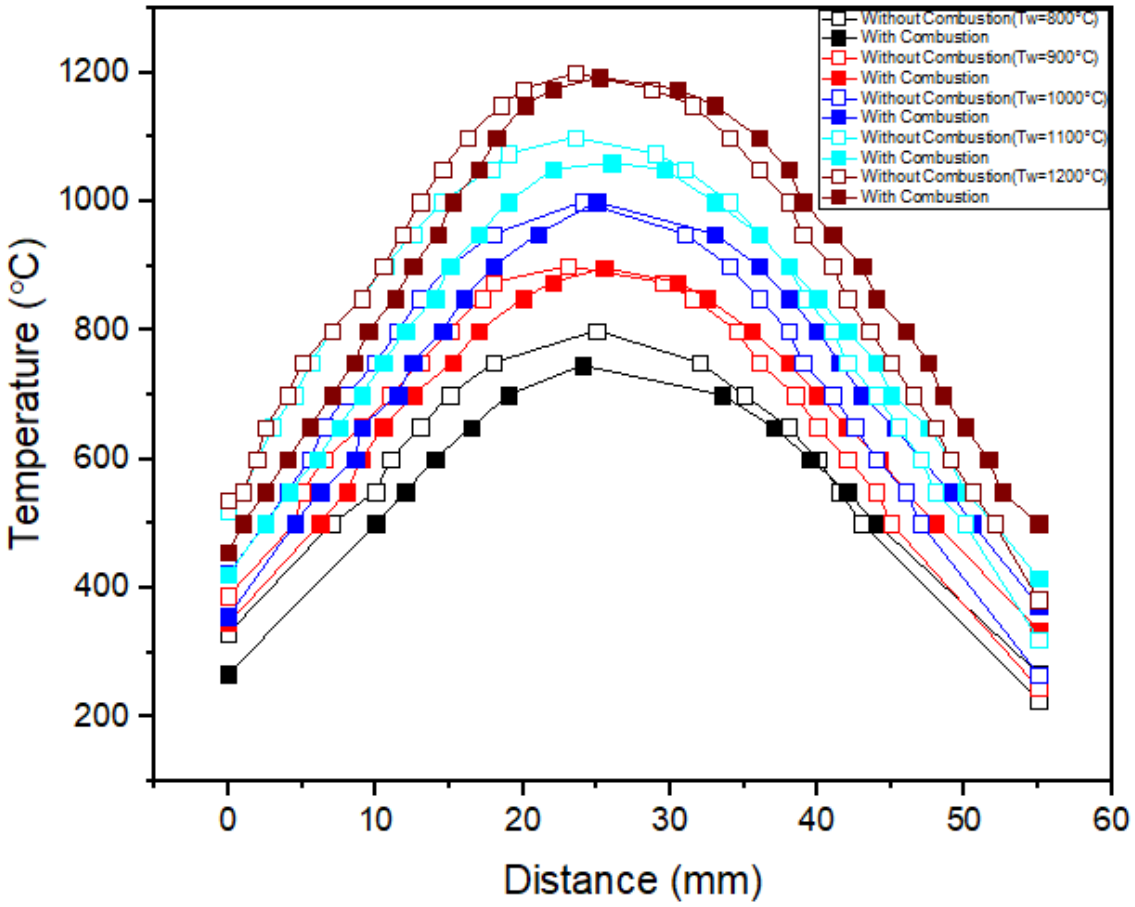

Figure 26: Reactor temperature profiles across the whole temperature's regime of interest at 100sccm (10sccm propane/air and 90sccm N_2).

4.2.4 Combined Temperature Profiles

All the temperature profiles at different flow rates were plotted. As shown in the diagrams, the peak temperature for the 10sccm and 10sccm propane/air with 90sccm nitrogen dilution was reached around 25mm of the reactor length, while for the 100sccm case, the maximum combustion temperature was reached at around 33mm for Tw=900. At 1000°C, the combustion temperature for 100sccm surpasses the nitrogen dilution case and at 1100°C, it even increases beyond the 10sccm case. The temperature profiles at 1200°C were very comparable to each other.

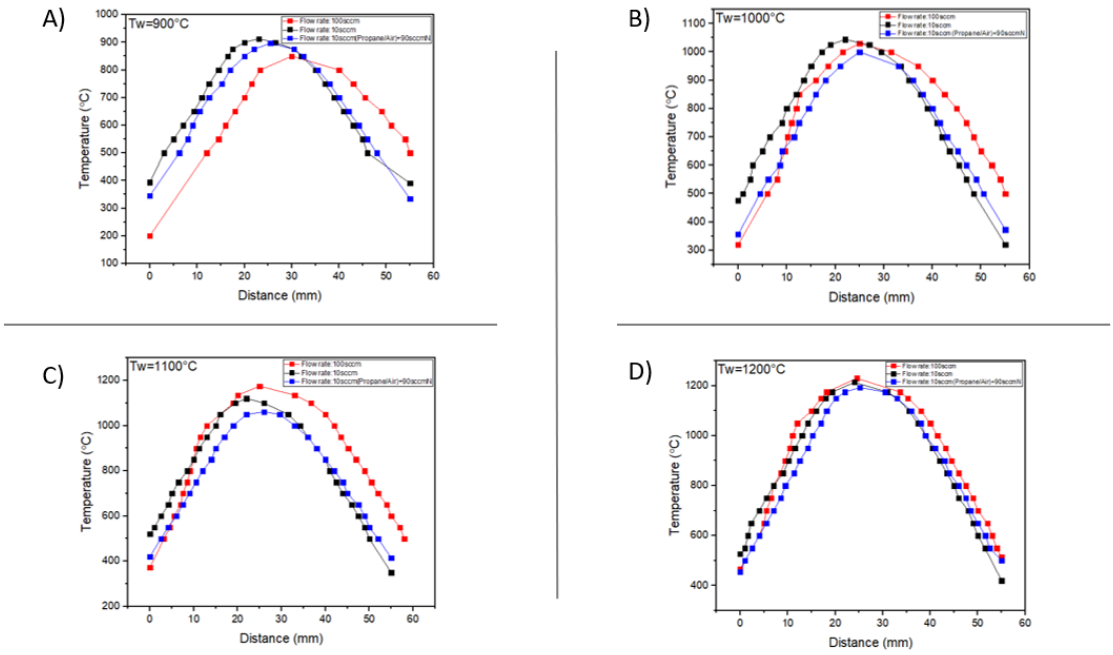

Figure 27: The temperature profiles comparison for different flow rates for the wall temperature A) 900°C, B) 1000°C, C) 1100°C and D) 1200°C.

4.3 Precursors Analysis (Gas Chromatography)

To set the premise for the results at low temperature, some GC analysis was needed to ascertain the gas composition as well as the precursor's analysis. There has been an effort in the past using almost the same experimental setup with a 3.6mm reactor and 20sccm flow rate [8].

To gain an insight into the exhaust gas composition for sooting vs non-sooting flames, the micro-combustion exhaust is investigated [8] for the temperature range of 750°C to 1000°C at an equivalence ratio of 2.5 and mixture flow rate of 20 sccm with the help of a GC. No soot was observed until 950°C. Soot was observed above 950°C and 1000°C. The H_2 concentration increases less steeply from 750°C to 800°C as compared to a drastic increase from 800°C to 900°C. From 900°C to 1000°C, there is a slight decrease in the H_2 concentration. Similarly, CO shows a similar trend, but the decrease in concentration from 900°C to 1000°C is more drastic than the decreases in

H_2 concentration. The maximum syngas is produced at 900℃. The CO_2 concentration increases slightly with increasing temperature because increasing temperature tends to shift the reaction towards complete oxidation to CO_2. Just when the CO concentration starts to drop, CO_2 concentration starts to rise because of complete oxidation at a higher temperature. The concentration profile of CH_4 decreases from 900℃ to 1000℃ because of increasing temperature. This increase in consumption of CH_4 at higher temperature corresponds to higher decomposition due to pyrolysis of fuel at high temperature, which produces more H_2 and C_2H_2[50] as evident from their concentration profiles in Fig. 28.

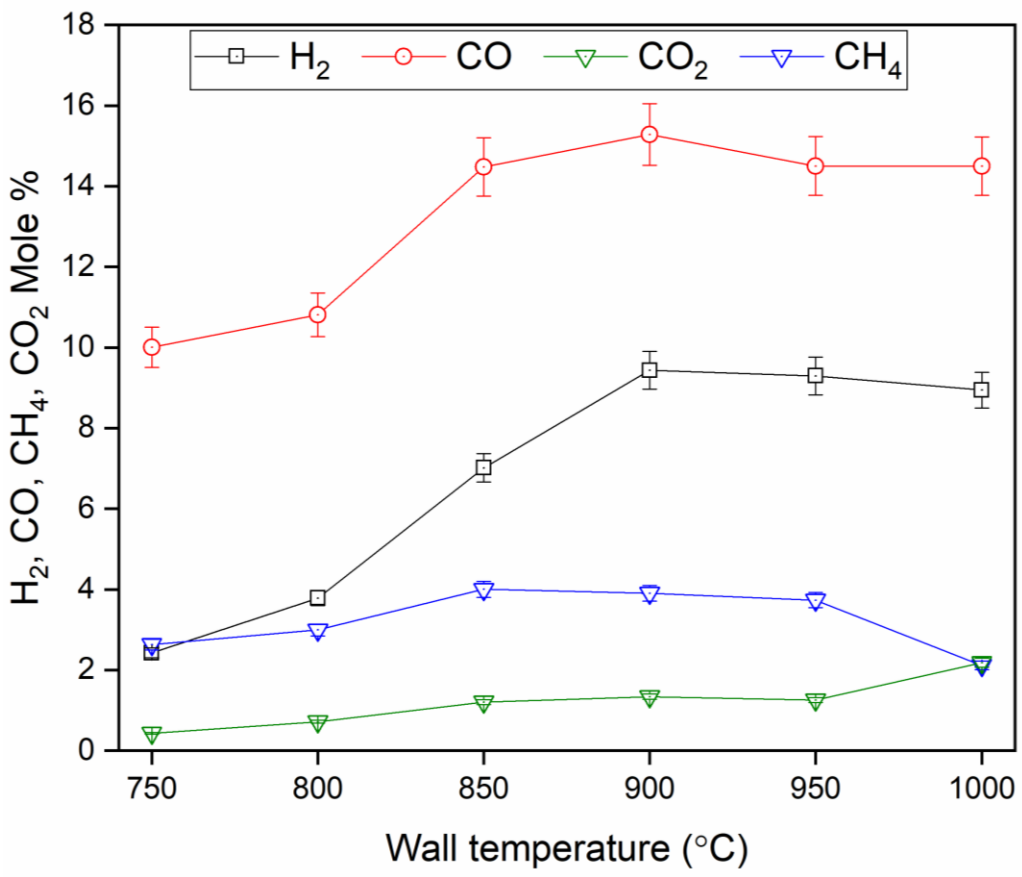

Figure 28: Exhaust species molar concentration at an equivalence ratio of 2.5 and a mass flow rate of 20sccm for different temperatures [8].

The temperature profiles of C_2 hydrocarbons in Fig. 29 shows a decreasing trend for the concentration of C_2H_6 and C_2H_4 with increasing temperature because the higher temperature promotes complete combustion. This happens because the propane oxidation proceeds from C_2H_6 through C_2H_4 to C_2H_2. It includes the abstraction of hydrogen by an oxidant, mainly OH, which forms hydrocarbon radical (vinyl) forming acetylene which is considered as the main precursor for the formation of aromatic hydrocarbons. It subsequently proceeds with a HACA [17] mechanism into heavier PAH and subsequently soot. As evident from the soot previously observed after 950℃ until 1000℃, it can be inferred that increased concentration of acetylene with increasing temperature acts as a dominant factor for soot formation observed in the results at 1000℃.

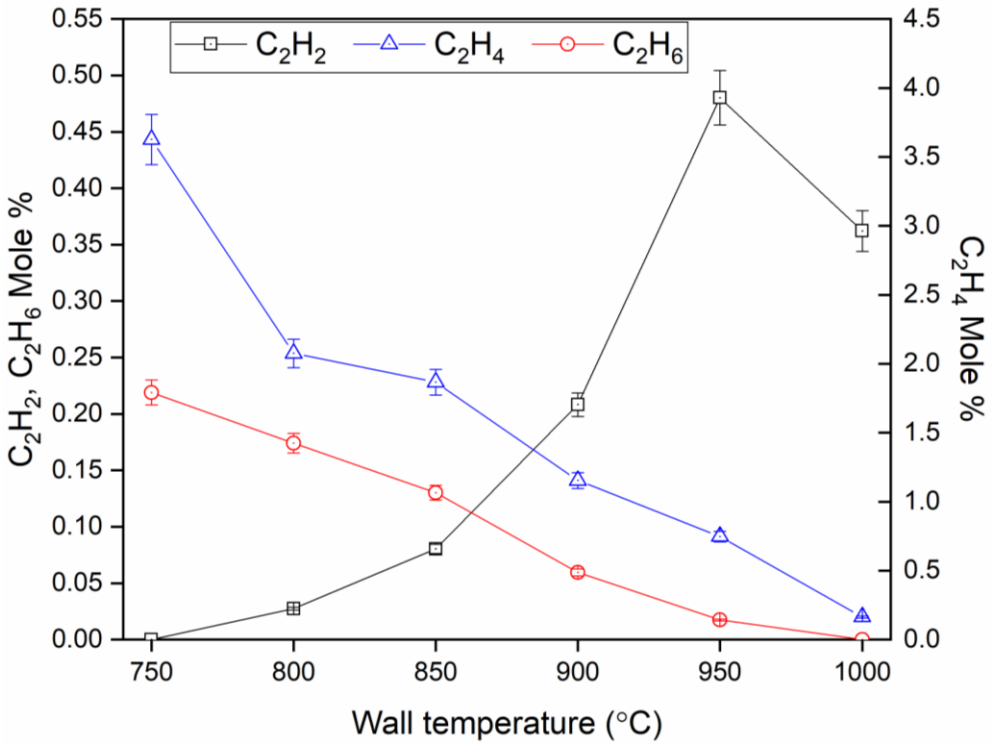

Figure 29: C_2 hydrocarbons concentration at an equivalence ratio of 2.5 and a mass flow rate of 20sccm for different temperatures [8].

These results give an insight into the results that we concluded from our visual soot analysis for our temperature regime of interest. No soot was observed until 950℃ even at higher equivalence ratios of 13, 50 or even 100 for a 100sccm case. Soot started appearing at 1000℃ at 2.5 for a flow rate of 10sccm (Fig. 14). Further increasing the temperature pushed the critical Φ to 3.7 as can be inferred from Fig. 30 because the acetylene concentration is decreasing from 950℃ to 1000℃. A similar trend was observed for a flow rate of 100sccm. Increasing temperature beyond 1100℃ might have triggered an increase in propane pyrolysis to acetylene, that's why the critical sooting equivalence ratio starts decreasing from 1100℃ to 1250℃. This needs further evidence in the form of more GC results at these temperatures.

The results for the nitrogen dilution case followed the same trend as previously observed for the sooting flames[19], i.e., increasing temperature decreases sooting as evident from Fig. 17. This needs further insight in the form of GC analysis.

CHAPTER 5

CONCLUSION

Soot poses serious threats to humans and the environment equally. This study was aimed at analyzing the effect of temperature on the critical sooting equivalence ratio and precursor formation in a micro-flow reactor with a controlled temperature profile, thereby devising ways to reduce soot. The effect of temperature on sooting limits of propane/air mixture at atmospheric pressure with temperatures ranging from 800-1250°C were investigated using a micro-flow reactor with a controlled temperature profile of diameter 2.3mm, equivalence ratios of 1-13 and inlet total flow rates of 10sccm, 100ssccm and 100sccm (10sccm propane/air with 90sccm of N_2). A resistive heating element was used as a heat source which was wrapped around the quartz tube reactor.

No soot was observed for all the flow rates at temperatures below 950°C at an equivalence ratio as high as 13. In the case of 100sccm total flow rate, no soot was observed from 700-950°C with an equivalence ratio as high as 50 and 100. The critical sooting equivalence ratio profiles for 10 and 100sccm were quite comparable in terms of the trend that they followed with the temperature beyond 1000°C. It increases steeply until 1050°C with a maximum at 1100°C and takes a steep dip until 1150°C and 1250°C. This is due to a decrease in acetylene concentration at a temperature above 1000°C as shown in Fig. 30 and after 1100°C, higher temperature might have triggered propane oxidation which in turn increases acetylene concentration thus decreasing critical sooting equivalence ratio. The critical sooting equivalence ratios at 10sccm were higher for the same temperature than the 100sccm. This was a counter-intuitive result as usually decreasing the residence time help push the critical Φ

further, but in this case, decreasing the residence time, in turn, has decreased the critical Φ.

The addition of nitrogen reduces the residence time as well as the temperature inside the reactor, both of these processes are known to increase the critical sooting equivalence ratios. The difference between the 10sccm, 100sccm and nitrogen dilution is large at 1000°C and limited at 1200°C. Thus the addition of inert diluents can be helpful in further reducing the total soot yield as well as increasing the critical sooting equivalence ratio. However, more work is needed to better account for the reaction temperature as the effect of diluents may be small compared to temperature.

A micro-flow reactor with a controlled temperature profile has been successfully demonstrated to study the temperature dependence of critical sooting equivalence ratio and precursors formation for propane/air mixture. Also, the dependence of critical sooting equivalence ratio on the residence time as well as the addition of inert diluent (nitrogen) has been demonstrated. Future work includes the detailed gas chromatography analysis of the exhaust gas composition and precursors. Also, improvements in the measurement of the reactions temperature profile during combustion is necessary to explain the results more vigorously, because introducing a thermocouple inside the combustion zone perturb the flow, thus reducing the accuracy of the results.

BIBLIOGRAPHY

[1] T.R. Barfknecht, Toxicology of soot, Prog. Energy Combust. Sci. 9 (1983) 199–237. doi:10.1016/0360-1285(83)90002-3.

[2] K.H. Homann, H.G. Wagner, Chemistry of carbon formation in flames, Proc. R. Soc. London. Ser. A. Math. Phys. Sci. 307 (1968) 141–152. doi:10.1098/rspa.1968.0180.

[3] L.A. Kennedy, J.P. Bingue, A. V. Saveliev, A.A. Fridman, S.I. Foutko, Chemical structures of methane-air filtration combustion waves for fuel-lean and fuel-rich conditions, Proc. Combust. Inst. 28 (2000) 1431–1438. doi:10.1016/S0082-0784(00)80359-8.

[4] H.G. Wagner, Soot formation in combustion, Symp. Combust. 17 (1979) 3–19. doi:10.1016/s0082-0784(79)80005-3.

[5] C.A. Pope, D.W. Dockery, Health effects of fine particulate air pollution: Lines that connect, J. Air Waste Manag. Assoc. 56 (2006) 709–742. doi:10.1080/10473289.2006.10464485.

[6] D. Koch, J. Hansen, Distant origins of Arctic black carbon: A Goddard Institute for Space Studies ModelE experiment, J. Geophys. Res. D Atmos. 110 (2005) 1–14. doi:10.1029/2004JD005296.

[7] H. Nakamura, R. Tanimoto, T. Tezuka, S. Hasegawa, K. Maruta, Soot formation characteristics and PAH formation process in a micro flow reactor with a controlled temperature profile, Combust. Flame. 161 (2014) 582–591. doi:10.1016/j.combustflame.2013.09.004.

[8] R.J. Milcarek, H. Nakamura, T. Tezuka, K. Maruta, J. Ahn, Microcombustion for micro-tubular flame-assisted fuel cell power and heat cogeneration, J. Power. 413 (2018) 191–197. doi:10.1016/j.jpowsour.2018.12.043.

[9] K. Maruta, Micro and mesoscale combustion, Proc. Combust. Inst. 33 (2011) 125–150. doi:10.1016/j.proci.2010.09.005.

[10] M. Frenklach, D.W. Clary, W.C. Gardiner, S.E. Stein, Detailed kinetic modeling of soot formation in shock-tube pyrolysis of acetylene, Symp. Combust. 20 (1985) 887–901. doi:10.1016/S0082-0784(85)80578-6.

[11] K. Kashiwa, T. Kitahara, M. Arai, Y. Kobayashi, Benzene pyrolysis and PM formation study using a flow reactor, Fuel. 230 (2018) 185–193. doi:10.1016/j.fuel.2018.04.009.

[12] P. Ghose, J. Patra, A. Datta, A. Mukhopadhyay, Effect of air flow distribution on soot formation and radiative heat transfer in a model liquid fuel spray combustor firing kerosene, Int. J. Heat Mass Transf. 74 (2014) 143–155.

doi:10.1016/j.ijheatmasstransfer.2014.03.001.

[13] K.P. Schug, Y. Manheimer-Timnat, P. Yaccarinc, I. Glassman, Sooting Behavior of Gaseous Hydrocarbon Diffusion Flames and the Influence of Additives, Combust. Sci. Technol. 22 (1980) 235–250. doi:10.1080/00102208008952387.

[14] P. Chemic, W. German, C24H , 2 /. J, 7 (1981).

[15] B.S. Haynes, H. Jander, H.G. Wagner, Optical Studies of Soot-Formation Processes in Premixed Flames, Berichte Der Bunsengesellschaft Für Phys. Chemie. 84 (1980) 585–592. doi:10.1002/bbpc.19800840613.

[16] J.J. Macfarlane, F.H. Holderness, F.S.E. Whitcher, Soot formation rates in premixed C5 and C6 hydrocarbonair flames at pressures up to 20 atmospheres, Combust. Flame. 8 (1964) 215–229. doi:10.1016/0010-2180(64)90067-7.

[17] V. V Kislov, A.I. Sadovnikov, A.M. Mebel, Formation Mechanism of Polycyclic Aromatic Hydrocarbons beyond the Second Aromatic Ring, J. Phys. Chem. A. 117 (2013) 4794–4816. doi:10.1021/jp402481y.

[18] B. Singh, W.E. Lear, Soot Formation in Combustion, 59 (1994) 2–5. doi:10.1007/978-3-642-85167-4.

[19] R.C. Millikan, Non-equilibrium soot formation in premixed flames, J. Phys. Chem. 66 (1962) 794–799. doi:10.1016/j.disc.2006.04.042.

[20] K.G. Neoh, J.B. Howard, A.F. Sarofim, Soot Oxidation in Flames, in: Part. Carbon, Springer US, Boston, MA, 1981: pp. 261–282. doi:10.1007/978-1-4757-6137-5_9.

[21] F. TAKAHASHI, I. GLASSMAN, Sooting Correlations for Premixed Flames, Combust. Sci. Technol. 37 (1984) 1–19. doi:10.1080/00102208408923743.

[22] C.P. Fenimore, Oxidation of soot by hydroxyl radicals, J. Phys. Chem. 71 (1967) 593–597. doi:10.1021/j100862a021.

[23] P. Desgroux, A. Faccinetto, X. Mercier, T. Mouton, D. Aubagnac Karkar, A. El Bakali, Comparative study of the soot formation process in a “nucleation” and a “sooting” low pressure premixed methane flame, Combust. Flame. 184 (2017) 153–166. doi:10.1016/j.combustflame.2017.05.034.

[24] B.R. Stanmore, J.F. Brilhac, P. Gilot, The oxidation of soot: A review of experiments, mechanisms and models, Carbon N. Y. 39 (2001) 2247–2268. doi:10.1016/S0008-6223(01)00109-9.

[25] P.F. Knewstubb, T.M. Sugden, Mass spectrometry of the ions present in

hydrocarbon flames, in: Symp. Combust., 1958: pp. 247–253. doi:10.1016/S0082-0784(58)80048-X.

[26] J.M. Singer, J. Grumer, Carbon formation in very rich hydrocarbon-air Flames-I. Studies of chemical content, temperature, ionization and particulate matter, in: Symp. Combust., 1958: pp. 559–569. doi:10.1016/S0082-0784(58)80092-2.

[27] H.F. Calcote, D.B. Olson, D.G. Keil, Are Ions Important in Soot Formation ?, Energy and Fuels. 2 (1988) 494–504. doi:10.1021/ef00010a016.

[28] J.L. Delfau, P. Michaud, A. Barassin, Formation of small and large positive ions in rich and sooting low-pressure ethylene and acetylene premixed flames, Combust. Sci. Technol. 20 (1979) 165–177. doi:10.1080/00102207908946906.

[29] B.S. Haynes, H. Jander, H.G. Wagner, The effect of metal additives on the formation of soot in premixed flames, Symp. Combust. 17 (1979) 1365–1374. doi:10.1016/S0082-0784(79)80128-9.

[30] P.J. Mayo, F.J. Weinberg, On the Size, Charge and Number-Rate of Formation of Carbon Particles in Flames Subjected to Electric Fields, Proc. R. Soc. A Math. Phys. Eng. Sci. 319 (2006) 351–371. doi:10.1098/rspa.1970.0183.

[31] K. Müller-Dethlefs, A.F. Schlader, The effect of steam on flame temperature, burning velocity and carbon formation in hydrocarbon flames, Combust. Flame. 27 (1976) 205–215. doi:10.1016/0010-2180(76)90023-7.

[32] A.G. Gaydon, H.G. Wolfhard, Flames: Their structure, radiation and temperature, Phys. Today. 24 (1971) 54. doi:10.1063/1.3022389.

[33] A.G. Gaydon, Continuous spectra inflames: the role of atomic oxygen in combustion, Proc. R. Soc. London. Ser. A. Math. Phys. Sci. 183 (1944) 111–124. doi:10.1098/rspa.1944.0024.

[34] U. Bonne, K.H. Homann, H.G.G. Wagner, Carbon formation in premixed flames, in: Symp. Combust., 1965: pp. 503–512. doi:10.1016/S0082-0784(65)80197-7.

[35] C. Boman, D. Böstrom, M. Öhman, Effect of fuel additive sorbents (kaolin and calcite) on aerosol particle emission and characteristics during combustion of pelletized woody biomass, 16th Eur. Biomass Conf. Exhebition. (2008) 1514–1517.

[36] K.C. Salooja, Combustion control by novel catalytic means, Nature. 240 (1972) 350–351. doi:10.1038/240350a0.

[37] D.H. Cotton, N.J. Friswell, D.R. Jenkins, The suppression of soot emission from flames by metal additives, Combust. Flame. 17 (1971) 87–98.

doi:10.1016/S0010-2180(71)80142-6.

[38] A. Feugier, Effect of Metal Additives on the Amount of Soot Emitted by Premixed Hydrocarbon, Adv. Chem. (1978). doi:10.1111/j.1475-3588.2008.00498.x.

[39] B.S. Haynes, H. Jander, H. Mätzing, H.G. Wagner, The influence of gaseous additives on the formation of soot in premixed flames, Symp. Combust. 19 (1982) 1379–1385. doi:10.1016/S0082-0784(82)80314-7.

[40] Ü.Ö. Köylü, C.S. Mcenally, D.E. Rosner, L.D. Pfefferle, Simultaneous measurements of soot volume fraction and particle size / microstructure in flames using a thermophoretic sampling technique, Combust. Flame. 110 (1997) 494–507. doi:10.1016/S0010-2180(97)00089-8.

[41] S. Will, S. Schraml, K. Bader, A. Leipertz, Performance characteristics of soot primary particle size measurements by time-resolved laser-induced incandescence, Appl. Opt. 37 (1998) 5647. doi:10.1364/ao.37.005647.

[42] T. Ni, J.A. Pinson, S. Gupta, R.J. Santoro, Two-dimensional imaging of soot volume fraction by the use of laser-induced incandescence, Appl. Opt. 34 (1995) 7083. doi:10.1364/ao.34.007083.

[43] F. Takahashi, I. Glassman, Comments on "Influence of temperature and hydroxyl concentration on incipient soot formation in premixed flames," by M. M. Harris, G. B. King, and N. M. Laurendeau, Combust. Flame. 67 (1987) 267–268. doi:10.1016/0010-2180(87)90103-9.

[44] M. Frenklach, M.K. Ramachandra, R.A. Matula, Soot formation in shock-tube oxidation of hydrocarbons, Symp. Combust. 20 (1985) 871–878. doi:10.1016/S0082-0784(85)80576-2.

[45] T.S. Wang, R.A. Matula, R.C. Farmer, Combustion kinetics of soot formation from toluene, Symp. Combust. 18 (1981) 1149–1158. doi:10.1016/S0082-0784(81)80119-1.

[46] C.P. Leusden, N. Peters, Experimental and numerical analysis of the influence of oxygen on soot formation in laminar counterflow flames of acetylene, Proc. Combust. Inst. 28 (2000) 2619–2625. doi:10.1016/S0082-0784(00)80680-3.

[47] B. Shukla, M. Koshi, A highly efficient growth mechanism of polycyclic aromatic hydrocarbons., Phys. Chem. Chem. Phys. 12 (2010) 2427–37. doi:10.1039/b919644g.

[48] M. Frenklach, A.D.D.W. Clary, S.E. Stein, Detailed kinetic modeling of soot formation in shock-tube pyrolysis of acetylene, (1984) 887–901.

[49] F. Zhao, W. Yang, W. Yu, H. Li, Y.Y. Sim, T. Liu, K.L. Tay, Numerical study of soot particles from low temperature combustion of engine fueled with diesel fuel and unsaturation biodiesel fuels, Appl. Energy. 211 (2018) 187–193. doi:10.1016/j.apenergy.2017.11.056.

[50] M. Alfè, B. Apicella, J.N. Rouzaud, A. Tregrossi, A. Ciajolo, The effect of temperature on soot properties in premixed methane flames, Combust. Flame. 157 (2010) 1959–1965. doi:10.1016/j.combustflame.2010.02.007.